

Review Article

JSUM Ultrasound Elastography Practice Guideline Liver

Masatoshi Kudo^{1*}, Tsuyoshi Shiina², Fuminori Moriyasu³, Hiroko Iijima⁴, Ryosuke Tateishi⁵, Norihisa Yada¹, Kenji Fujimoto^{6, 7}, Hiroyasu Morikawa⁸, Masashi Hirooka⁹, Yasukiyo Sumino¹⁰, Takashi Kumada¹¹

1. Department of Gastroenterology and Hepatology, Kinki University School of Medicine, Osaka-sayama, Osaka, Japan
2. Human Health Sciences, Graduate School of Medicine, Kyoto University, Kyoto, Japan
3. Department of Gastroenterology and Hepatology, Tokyo Medical University, Tokyo, Japan
4. Department of Internal Medicine, Hyogo College of Medicine, Nishinomiya, Hyogo, Japan
5. Department of Gastroenterology, Graduate School of Medicine, the University of Tokyo, Tokyo, Japan
6. Department of Internal Medicine, Nagayama Hospital, Kumatori, Osaka, Japan
7. Division of Clinical Research, ONH Minamiwakayama Medical Center, Tanebe, Wakayama, Japan
8. Department of Hepatology, Graduate School of Medicine, Osaka City University, Osaka, Japan
9. Ehime University Graduate School of Medicine, Department of Gastroenterology and Metabology, Toon, Ehime, Japan
10. Division of Gastroenterology and Hepatology, Toho University Ohmori Medical Center, Tokyo, Japan
11. Department of Gastroenterology and Hepatology, Ogaki Municipal Hospital, Ogaki, Gifu, Japan

Abstract

In diffuse liver disease, it is extremely important to make an accurate diagnosis of liver fibrosis prior to determining indications for therapy or predicting treatment outcome and malignant potential. Although liver biopsy has long been the gold standard in the diagnosis of liver fibrosis, it is still an invasive method. In addition, the sampling error is an intrinsic problem of liver biopsy. Non-invasive serological methods for the diagnosis of liver fibrosis can be affected by factors unrelated to the liver. Recently, after the introduction of FibroScan, it has become possible to measure liver fibrosis directly and non-invasively by elastography, which has attracted attention as a non-invasive imaging diagnostic tool for liver fibrosis. In addition, Real-time Tissue Elastography is currently being used to conduct clinical trials at many institutions. Moreover, Virtual Touch Quantification enables the observation of liver stiffness at any location by simply observing B-mode images. Furthermore, the recently developed ShearWave Elastography visualizes liver stiffness on a color map. Elastography is thought to be useful for all types of diffuse liver diseases. Because of its association with portal hypertension and liver carcinogenesis, elastography is expected to function as a novel prognostic tool for liver disease. Although various elastographic devices have been developed by multiple companies, each device has its own measurement principle, method, and outcome, creating confusion in clinical settings. Therefore, it is extremely important to understand the characteristics of each device in advance. The objective of this guideline, which describes the characteristics of each device based on the latest knowledge, is for all users to be able to make the correct diagnosis of hepatic fibrosis by ultrasound elastography.

Keyword

elastography, elasticity, shear wave, stiffness, strain

1. Preamble

In diffuse liver disease, it is extremely important to make an accurate diagnosis of liver fibrosis prior to determining indications for antiviral therapy or predicting treatment outcome and malignant potential. Although liver biopsy has long been the gold standard in the diagnosis of liver fibrosis, it is still an invasive method with potential bleeding and severe pain. In addition, the sampling error is the intrinsic problem of liver biopsy because of the small sampling size, and diagnostic consistency may be influenced by inter observer variability. There have been many reports of non-invasive serological methods for the diagnosis of liver fibrosis, including the use of serum markers of liver fibrosis (such as platelet, hyaluronic acid, and type IV collagen 7S domain), aminotransferase/platelet ratio index (APRI), and algorithm-based serum models (such as FibroIndex, FIB-4, and FibroTest). However, these methods can be affected by factors unrelated to the liver.

Elastography, developed as a non-invasive tool to measure tissue elasticity, has advanced particularly in the field of breast cancer. Recently, it has become possible to measure liver fibrosis directly and non-invasively by elastography, which has attracted attention as a non-invasive imaging diagnostic tool for liver fibrosis. Especially after the introduction of FibroScan, a device to measure the stiffness of liver, the application of elastography for the measurement of liver stiffness has been investigated. In addition, Real-time Tissue Elastography, i.e., the world's first practical ultrasound (US) elastographic technology developed in Japan, is currently being used to conduct clinical trials at many institutions. Moreover, Virtual Touch Quantification, in which constant pressure exerted by focused US generates a shear wave, enables the observation of liver stiffness at any location by simply observing B-mode images. With this technology, it is possible to examine cases with ascites retention for which FibroScan is not useful. Furthermore, a recently developed ShearWave Elastography visualizes liver stiffness on a color-map. Although elastography has been used mostly to examine viral liver disease, non-alcoholic fatty liver disease (NAFLD), autoimmune hepatitis, drug-induced liver injury, and alcoholic liver disease, the technology is thought to be useful for all types of diffuse liver diseases, such as primary biliary cirrhosis, Budd-Chiari syndrome, and idiopathic portal hypertension. Because of its association with portal hypertension and liver carcinogenesis, elastography is expected to function as a novel prognostic tool for liver disease. Although various elastographic devices have been developed by multiple companies, each device has its own measurement principle, method, and outcome, creating confusion in clinical settings. Therefore, it is extremely important to understand the characteristics of each device in advance.

In this guideline, we provide the latest knowledge and understanding of elastographic devices, particularly those widely used for the diagnosis of liver fibrosis.

2. Characteristics of each device

US elastography is categorized into four groups based on the excitation method and measurement quantity as described in the Basics and Terminology part. We will discuss the devices that are currently used to diagnose liver fibrosis.

- 1 **Strain elastography: Hitachi, Siemens, GE, and Toshiba**
- 2 **Acoustic Radiation Force Impulse (ARFI) imaging: Siemens**
- 3 **Point shear wave elastography: Siemens and Philips**
- 4 **Shear wave elastography: SuperSonic Imagine and Siemens**
- 5 **Transient shear wave elastography: FibroScan**

2.1. Strain imaging

2.1.1. Strain elastography

2.1.1.1. Real-time Tissue Elastography (Hitachi)

A) Introduction

Commercialized by Japanese companies using technology developed in Japan, Real-time Tissue Elastography® (RTE) is the world's first practical imaging modality for the diagnosis of tissue elasticity. RTE belongs to the category of Strain elastography and visualizes tissue deformation, or strain, caused by manual compression or heartbeat. With RTE, relative tissue strain is displayed on conventional B-mode images in real-time. Areas with lower strain (relatively hard tissue) and those with higher strain (relatively soft tissue) in the region of interest (ROI) are displayed in blue and red, respectively, with a 256-color gradation (Fig. 1, 2)¹⁻³.

B) Indication

RTE is indicated for various diffuse liver diseases, including virus liver disease²⁻⁹, NAFLD¹⁰, autoimmune hepatitis, primary biliary liver disease, alcoholic liver disease, and drug-induced liver injury. RTE is also reportedly useful for the diagnosis of portal hypertension¹¹. In addition, the usefulness of RTE in the prognosis of liver cancer is currently being investigated in a multicenter study.

C) Procedures (including Tips and Tricks)

RTE application software can be loaded by different US imaging devices from Hitachi Aloka Medical (Tokyo, Japan), including but not limited to HI VISION Ascendus, HI VISION Preirus, HI VISION Avius, Noblus, HI VISION 900, EUB-8500, EUB-7500. Imaging is performed with a 7-3 MHz linear probe (EUP-L52).

1) Scanning method^{2-4, 7-9}

Successful RTE imaging depends on the clarity of B-mode images—the fundamental US images—and therefore, B-mode images need to be void of artifacts.

1. Visualize the right hepatic lobe from the right intercostal space of a patient in the supine position

with the right arm elevated to make the intercostal space wider.

2. Place a probe lightly against the skin without vibration.
3. Select an extraction point at which B-mode images are void of artifacts.
4. Try to obtain images displaying vertical, not horizontal, strain by placing the probe to generate an echo beam in the direction of the heart.
5. While the patient is lightly holding breath, make sure that RTE images are displayed periodically by cardiac motion.

2) ROI setup

The ROI can be established in two ways: Place the ROI only inside the liver^{2-4, 7-9, 12} or place it over the liver and the surrounding tissue, such as subcutaneous and/or muscle layer^{13, 14}. In the latter case, however, color distribution on RTE images changes depending on the ratio between the liver and the surrounding tissue in the ROI because RTE displays relative tissue strain. Accordingly, any inappropriate area or object should be excluded from the ROI to avoid introducing artifacts. Placing ROI inside the liver is the key to generate uniform images of the entire liver^{3, 7, 9, 15}. Although selecting a large ROI area with presumably no or few artifacts can result in successful imaging, it is difficult to avoid large blood vessels if ROI is too large. For this reason, a 2.5×2.5 -cm square ROI is often used^{8, 9}.

1. Avoid large blood vessels (to eliminate artifacts from the anechoic area) (Fig. 3a)
2. Avoid the area near the ribs because the acoustic shadow will be displayed in blue on US images (Fig. 3b).
3. Avoid the surface of the liver because it is often displayed in blue due to multiple reflection echo (Fig. 3c).
4. Avoid areas deep inside the liver because they often appear blue due to poor ultrasound penetration (Fig. 3d).

3) When having trouble with observation

1. Try another intercostal space
2. Select an intercostal space which is softer and has a thinner subcutaneous layer
3. Avoid including body organs under the subcutaneous layer, such as ribs and lungs, in imaging

4) Selection of frames for analysis

1. Select frames with strain generated in the direction of depth
2. Select frames with no artifacts
3. Good images may be obtained in the end of left ventricular diastole in electrocardiographic gating or at the largest downward wave on a strain graph (Fig. 4).

D) Results (What do the values mean?)

In chronic hepatitis, the liver tissue hardens unevenly as fibrosis advances. Accordingly, if the ROI is placed only over the liver, it will enhance the color variation of RTE images, increasing areas with

relatively low strain (blue area). This results in the generation of images with a mottled appearance (Fig. 5)^{2,4,9}. Using a mechanical model of fibrosis progression in basic research, Shiina et al. showed that areas with low strain increase as fibrosis progresses, and strain distribution becomes complex, as shown in clinical cases¹⁶.

1) Subjective evaluation method

Because Liver Elasticity Score, obtained by visual assessment of low strain areas (blue area) on RTE images (Fig. 6), are positively correlated with fibrosis progression and the level of type-4 collagen 7S (Figs. 7, 8)⁴, these scores are useful for the diagnosis of liver fibrosis.

However, because examiner subjectivity influences Liver Elasticity Score, more objective evaluation methods are needed.

2) Objective evaluation methods

Examiner subjectivity and past experiences influence the outcome of visual assessment. To overcome this problem, various quantitative methods have been developed to objectively assess tissue elasticity. Here, we discuss image pattern recognition and strain-ratio calculation.

● Image pattern recognition

Parameters obtained by adjusting grayscale, histogram, and binarization are called feature values, and these values are used in pattern recognition. In RTE imaging, feature values obtained by the US device itself or by separate imaging software can be used to calculate a correlation with liver fibrosis. The degrees of strain are converted to feature values using 256 color gradations with blue being 0 and red being 255.

Tatsumi et al. and Morikawa et al. have reported that mean relative strain values (MEAN) inversely correlated with liver stiffness and fibrosis in patients with chronic hepatitis C (Figs. 9, 10). On the other hand, the standard deviation of relative strain values (SD), the percentage of low strain area (percentage of blue color area – %AREA), and the complexity of the low strain (blue) area (calculated as $\text{perimeter}^2/\text{area}$ – COMP) were positively correlated with liver stiffness and fibrosis (Figs. 9-11)^{2,7}.

➤ Calculation of function values

Some methods use feature values as an independent variable to perform multiple regression and principal component analysis to calculate the function values.

a. Liver Fibrosis Index

Fujimoto et al. performed RTE imaging of 295 patients with chronic hepatitis C and cirrhosis and 15 healthy individuals (310 cases in total) and extracted 9 feature values: MEAN, SD, %AREA, COMP, the skewness (SKEW) and kurtosis (KURT) of the histogram, and the homogeneity (entropy, or ENT), complexity (inverse differential moment, or IDM), and uniformity (angular second moment, or ASM) of texture. The authors used the 9 feature values as independent variables and the histological

fibrosis (F) stage as dependent variables in multiple regression analysis to calculate Liver Fibrosis Index (LF Index)^{5, 8}.

In a validation study of LF Index using 245 patients with cirrhosis and chronic hepatitis B and C, Yada et al. observed significant differences between F0-F1 and F4, F2 and F4, and F3 and F4 (Fig. 12). The sensitivity, specificity, and accuracy of diagnosis were as high as 73.5%, 79.7%, and 78.3% for F4; 78.4%, 80.2%, and 79.6% for F3 or higher; 70.0%, 76.4%, and 73.0% for F2 or higher. The AUROC (Area Under the Receiver Operating Characteristic) were also high, with the corresponding values of 0.946, 0.865, and 0.800 (Fig. 13)⁹.

b. Elasticity index

Wang et al. examined 55 chronic hepatitis B patients and 10 healthy individuals and used the feature values as independent variables to perform principal component analysis. Four types of principal components extracted from the analysis were used as integrative functions to calculate an elasticity index. They found a significant correlation between the elasticity index and liver fibrosis ($p < 0.001$) (Fig. 14), and the AUROC was 0.93 for F1 or above ($p < 0.001$), 0.92 for F2 or above ($p < 0.001$), 0.84 for F3 or above ($p < 0.05$), and 0.66 for F4 ($p > 0.05$)¹⁷.

● Strain ratios

There are two types of evaluation methods that use the strain ratio in analysis. The mainstream method places the ROI only in liver parenchyma for analysis and calculates the ratio between the parenchyma and blood vessel. In another method, the ROI includes liver parenchyma and the surrounding tissue, and the strain ratio between the two tissues is used in the analysis.

Koizumi et al. performed imaging of 70 chronic hepatitis C patients with the ROI placed only in liver parenchyma, and they used the strain ratio (elastic ratio, Fig. 15) between the liver parenchyma and the peripheral hepatic vein for evaluation. Elastic ratios increased with the progression of liver fibrosis, from a ratio of 2.21 in F1 (95% confidence interval, 1.94–2.70), 2.69 in F2 (2.29–2.97), 3.42 in F3 (3.07–3.65), to 4.66 in F4 (4.40–4.93), with a significant positive correlation between the ratios and hepatic fibrosis ($r^2 = 0.82$, $p < 0.001$). In addition, there was a significant difference between F2 and F3 ($r^2 = 0.36$, $P = 0.02$) as well as F3 and F4 ($r^2 = 0.41$, $P = 0.001$); but, no significant difference was observed between F1 and F2 (Fig. 16). In addition, the elastic ratio was not correlated with inflammation ($p = 0.36$). The measurement results of two examiners showed a strong correlation ($r^2 = 0.869$, $p < 0.0001$), demonstrating that inter observer variability was extremely low (Fig. 17)⁶.

In a study using patients with NAFLD, Ochi et al. observed a significant correlation between elastic ratio and liver fibrosis. In addition, there was a significant difference in elastic ratios between patients with NAFLD activity score (NAS) ≤ 4 and those with the score ≥ 5 (Fig. 18)¹⁰.

● Other methods

Using hepatitis B and C patients, Friedrich-Rust et al. calculated tissue elasticity from every pixel in the RTE image and perform multivariate analysis to obtain a unique formula. Elasticity scores calculated using the formula showed a significant correlation with liver fibrosis, as with other analysis.

The authors also improved the diagnostic capability of the system for liver fibrosis by incorporating platelet counts and γ -glutamyl transpeptidase (GGT) (Fig. 19)¹⁸.

● Influences other than liver fibrosis

In a study of hepatitis C patients by Fujimoto et al., none of the feature values were correlated with inflammatory grade⁸ (Fig. 20). Moreover, in a validation study using chronic hepatitis B and C patients, Yada et al. observed no correlation between inflammatory grade and LF Index⁹. In addition to liver fibrosis, inflammation, jaundice, and blood congestion are known to affect shear wave imaging, such as FibroScan and Virtual Touch Quantification (VTQ)¹⁹⁻²². On the other hand, RTE can evaluate liver fibrosis without being affected by these factors.

E) Limitations

While FibroScan cannot be used in patients with ascites retention, RTE is able to perform measurements in such cases (Fig. 21)²³.

Various RTE imaging and analysis methods are currently available, and they all show a clear correlation with liver fibrosis. However, a comparative study is needed to reveal superiority among these methods. Although the technique that uses heartbeat is most popular today, weak pulsation can adversely affect the quality of RTE images. Moreover, even though RTE can be applied to most cases owing to its ability to assess patients with ascites retention and narrow intercostal spaces, it is difficult to generate clear RTE images of severely obese patients due to ultrasound attenuation. It is also necessary to learn tips and tricks to, for example, prevent artifacts. The experience and skills of examiners can influence the accuracy of ultrasonography; however, in liver RTE, variability among examiners with proper training is reportedly low⁶. To spread liver RTE and further improve accuracy, it is necessary to standardize the imaging and analysis methods and establish an effective RTE training system.

F) Recommendations

RTE is a tissue elasticity imaging method that has been put into practical use for the first time in the world.

In diffuse liver diseases, the hardness of hepatic tissue becomes irregular as liver fibrosis progresses. This can be seen as uneven, patchy color distribution on RTE images, with an increase in areas with relatively low strain (blue area). Such change can be easily observed visually; however, objective assessment can be made only by the use of LF Index and elastic ratio, or strain ratio.

RTE accurately measures liver fibrosis without adverse effects of ascites accumulation, inflammation, jaundice, and blood congestion.

Multicenter studies are currently being performed to compare RTE imaging results with histological findings in specimens obtained by resection and biopsy and also to use RTE as a non-invasive prognostic tool in, for example, esophageal varix and liver cancer incidence. We looked forward to the results of these studies.

eSie touch Elasticity Imaging (Siemens)

A) Introduction

This is a Strain elastography-based technology that uses the spatial correlation method to measure tissue strain caused by minute body movements such as breathing or heartbeat. An acquired image is superimposed onto a B-mode image and can be displayed side by side with the original B-mode image.

B) Indication

The efficacy of eSie Touch Elasticity Imaging for the diagnosis of fibrosis in diffuse liver disease has not been fully elucidated.

This technology has been used for the diagnosis of hepatic tumors, especially for the differential diagnosis between benign and malignant tumors.

C) Procedures (including Tips and Tricks)

Switch to the elasticity imaging mode and visualize the lesion while watching the B-mode image.

When evaluating tumors, both tumor and normal parenchyma should be displayed in the ROI.

Regardless of the size of the ROI, the system always uses an entire B-mode image to perform arithmetic processing for strain imaging. Therefore, the size and location of ROI can be altered, with the former as large as the size of the B-mode image, after obtaining a still image.

The ROI image is displayed in grayscale or color, and colors representing soft and hard tissues can be reversed. However, measurement of strain ratios is possible only when a grayscale image is displayed.

D) Results (What does the value mean?)

eSie Touch Elasticity Imaging has not been used extensively in the diagnosis of fibrosis in diffuse liver diseases.

The technology captures tumor homogeneity/heterogeneity as well as differences in elasticity between the tumor and the surrounding tissue as differences in relative strains (Fig. 22). Grayscale images are used to measure strain ratios to display the relative stiffness in the two regions numerically (Fig. 23).

E) Limitations

The efficacy of this technology for the diagnosis of fibrosis in diffuse liver disease has not been fully elucidated.

Although tissue at a depth of 16 cm can be visualized, images generated at such depth may not be reliable.

Imaging may not be successful in patients with difficulty in holding breath or in severely obese patients.

F) Recommendations

eSie Touch Elasticity Imaging is one of the Strain elastography methods using the spatial correlation method to measure tissue strain.

Neoplastic lesions can be evaluated as a relative tissue strain.

The number of studies using this technology is not sufficient for making a definitive conclusion. We look forward to further study results in the near future.

2.1.1.2. Elastography (Direct Strain Elastography) (GE)

A) Introduction

Direct strain elastography belongs to the category of Strain elastography and uses the revised direct strain method to measure tissue dislocation. The system assigns warm colors to a group of pixels representing strains higher than the mean value on the strain distribution graph and cool colors to a group of pixels representing lower strains, followed by the superimposition of the color-map on a conventional B-mode image in real-time (Fig. 24).

B) Indication

Diffuse liver diseases, hepatic tumors

C) Procedures (including Tips and Tricks)

Visualize the target area using B-mode

Push the “Elasto” button to start elastography mode

Set the ROI large enough to cover the target area

Apply gentle and steady pressure to the probe to maintain the quality bar or the quality graph at a high level

Elastography is also obtained by heartbeat. In this case, place a probe lightly against the skin without vibration.

Save the still image and/or video clip

To prevent calculation errors, artifacts should be avoided.

D) Results (What do values mean?)

The efficacy of this technology for the diagnosis of fibrosis in diffuse liver disease has not been fully elucidated.

In the case of neoplastic lesions, it is possible to capture tumor homogeneity/heterogeneity as well as differences in elasticity between the tumor and normal parenchyma as differences in relative strain.

Elasticity index and elasticity ratio are used in analysis.

Elasticity index: the numerical expression of strain on a color-coded strain image generated using the ROI. Higher values represent harder tissue.

Elasticity ratio: the ratio of elasticity indexes obtained as above.

E) Limitations

The efficacy of this technology for the diagnosis of fibrosis in diffuse liver disease has not been fully elucidated.

The system is not applicable to tumors located deep inside the liver where compression hardly reaches.

Imaging may not be successful in patients with difficulty in holding breath or in severely obese patients.

F) Recommendations

The number of studies on this technology is not sufficient for making a definitive conclusion. We look forward to further study results in the near future.

2.1.1.3. Elastography (Toshiba)

A) Introduction

This technology belongs to the category of Strain elastography and measure tissue displacement using tissue Doppler, with excellent real-time performance and relatively good signal-to-noise ratios. However, because of its angle-dependent nature, the system measures tissue displacement in a one-dimensional plane in the direction of the beams. In addition, the measurement of displacement which is larger than half the wavelength of the beam causes errors due to aliasing.

B) Indication

Diffuse liver diseases, hepatic tumors

C) Procedures (including Tips and Tricks)

A B-mode image is used to confirm that the target area is sufficiently compressed by manual compression.

When measuring liver stiffness using a compression technique, press the corresponding area iteratively by hand to make sure that tissue strain is observable on the screen. At this point, strain can be quantitated by comparing it with another organ with relatively uniform stiffness, such as a kidney, or by calculating strain values while manually applying constant pressure (Fig. 25). There is also a method of measuring strain pattern or strain caused by heartbeat.

To quantitatively measure liver stiffness in diffuse liver disease, constant pressure should be applied to the probe. The key to the compression method is to perform measurement at the maximum or minimum compression point. The velocity vector of compression is a near-sinusoidal wave. In addition, the area of interest needs to be compressed evenly for successful quantitation. The uniformity of measurement at multiple sites having uniform stiffness should be confirmed.

D) Results (What does the value mean?)

The use of a strain distribution map (unevenness on the strain image) may be able to diagnose the progression of liver fibrosis (has not been published) (Fig. 26).

When evaluating tumor stiffness, tissue stiffness of a tumor is calculated by comparing it with

normal parenchyma. In general, metastatic liver cancers have a high strain ratio.

E) Limitations

The efficacy of this technology for the diagnosis of fibrosis in diffuse liver disease has not been fully elucidated.

Aliasing may occur because the system uses the Doppler method.

F) Recommendations

This is one of the Strain elastography methods using the tissue Doppler method, and therefore, attention must be paid to aliasing.

At present, the number of studies using this technology is not sufficient for making a definitive conclusion. We look forward to further study results in the near future.

2.1.2. Acoustic Radiation Force Impulse (ARFI) imaging

2.1.2.1. Virtual Touch Imaging (Siemens)

A) Introduction

Virtual Touch™ imaging (VTI) uses acoustic radiation force impulse (ARFI) to compress tissue and thus cause tissue dislocation, which is measured to display relative tissue strains. The spatial correlation method is used to measure dislocation. The system is minimally operator-dependent because there is no requirement for manual compression.

VTI images, available in grayscale only, are displayed next to the original B-mode image (Fig. 27). Areas with lower strain appear in black and those with higher strain in white.

B) Indication

The efficacy of VTI for the diagnosis of fibrosis in diffuse liver disease has not been fully elucidated.

A previous study has also reported the efficacy of VTI in differential diagnosis between benign and malignant liver cancers²⁴.

C) Procedures (including Tips and Tricks)

Switch to the VTI mode.

Adjust the size and location of the ROI. Because of focus dependency, the size of ROI should not be excessively larger than the size of the tumor unless absolutely necessary, and place the focus near the bottom of the tumor.

Start imaging and keep the liver in place while acquiring the image.

D) Results (What does the value mean?)

The efficacy of this technology for the diagnosis of fibrosis in diffuse liver disease has not been fully elucidated.

VTI captures tumor homogeneity/heterogeneity as well as differences in elasticity between the tumor and normal parenchyma as differences in relative strains.

E) Limitations

The technology is applicable regardless of ascites retention.

Unlike Strain elastography, the screen freezes every time an image is acquired.

Imaging reliability is not displayed.

F) Recommendations

Because ARFI is used to compress tissue, VTI is operator independent.

At present, only a small number of studies have reported the use of VIT for the diagnosis of liver fibrosis in diffuse liver disease. We look forward to further reports in the future.

2.2. Shear wave imaging

2.2.1. Point shear wave elastography

2.2.1.1. Virtual Touch Quantification (Siemens)

A) Introduction

Virtual Touch™ quantification (VTQ) was the first commercially available ARFI-based elastography technique and is currently one of the most widely used elastography methods in Japan.

The shear wave propagation velocity in an object (elastic body) is positively correlated with the elastic modulus of the object. In other words, the faster the shear wave velocity traveling through the object, the harder the object. VTQ uses pulsed focused US (acoustic push pulse) to generate transverse elastic wave (shear wave) and uses tracking US pulses to measure the shear wave velocity and thus tissue stiffness. Convex or linear probes for diagnostic ultrasonography are used in VTQ. Shear waves are generated by irradiating biological tissue with push pulses with a duration of 200–300 μs, and shear wave velocity is calculated by measuring tissue dislocation through the transmission and reception of US pulses for B-mode imaging. A B-mode image for positioning and measurement results is displayed on the same screen (Fig. 28).

In VTQ, tissue stiffness is expressed by shear wave velocity, V_s [m/s].

$$V_s = \sqrt{\frac{E}{2(1+\gamma)\rho}}$$

V_s , velocity of shear wave; E , Young's modulus; γ , Poisson's ratio; ρ , density.

FibroScan measures shear wave velocity similarly to VTQ, but calculate the Young's modulus E [kPa] using the equation $E=3\rho V_s^2$ (tissue density, $\rho = 1 \text{ g/cm}^3$; shear wave velocity, V_s [m/s]). However, the system assumes that the deformation of an object does not cause any change in the volume (Poisson's ratio, $\gamma = 0.5$), and the density of liver is the same as the density of water (tissue density, $\rho = 1 \text{ g/cm}^3$). This may be reasonable for the liver with advanced fibrosis; however, the validity of this assumption in relation to other organs has not been fully elucidated, and Siemens has been using shear wave velocity, V_s [m/s], to characterize the properties, including stiffness.

B) Indication

VTQ is indicated for patients with chronic liver disease, particularly viral hepatitis²⁵⁻²⁸, requiring the diagnosis of liver fibrosis. Aggressive treatment is needed for patients with viral hepatitis, and VTQ is useful for patients contraindicated for liver biopsy.

VTQ is expected to be useful in the assessment of non-viral hepatitis such as non-alcoholic steatohepatitis²⁹⁻³², portal hypertension^{33,34}, esophageal varices¹⁶, and cancer prognosis.

C) Procedures (including Tips and Tricks)

Device: ACUSON S2000

Probe: Convex probe for abdominal imaging or linear probe for superficial imaging

In general, imaging is performed from the right intercostal space of a patient in the supine position holding a normal breath. Prolonged breath holding should be avoided because it will increase central

venous pressure, causing the values of V_s to increase. The probe is held lightly against the body, and while observing the B-mode image, a 0.6×1 cm ROI devoid of large blood vessels is placed 1–2 cm below the liver surface. Measurement is started by pushing the button and is repeated several times to obtain the mean or median V_s values. Imaging of the right hepatic lobe is recommended to be undertaken as possible, because imaging of the left hepatic lobe is often influenced by the movement of body organs, such as the heart, lungs, diaphragm, and stomach (Fig. 29)³⁵.

Tips and Tricks for generating stable focused US

1. Place the ROI 1–2 cm below the liver surface
2. Press the probe parallel to the liver surface
3. Make sure that no large vessels or other objects, such as space occupying lesion, are present between the ROI and probe.

D) Results (What does the value mean?)

* Measurement results are expressed as X.XX kPa if the reliability is low.

V_s values reportedly increase with the progression of liver fibrosis. The diagnostic sensitivity of VTQ is reportedly similar to the sensitivity of FibroScan^{25, 28, 36}.

In a previous study investigating the diagnostic capability of VTQ in chronic hepatitis C and B patients, Friedrich-Rust et al. used the cut-off value of 1.75 m/s and obtained the sensitivity of 81.8%, the specificity of 91.5%, a positive predictive value of 78.3%, and a negative predictive value of 93.1%²⁵. The AUC for fibrosis of F2 or above was 0.82 (95% confidence interval, 0.73–0.91) in VTQ, 0.84 (0.75–0.93) in FibroScan, 0.82 (0.75–0.93) in FibroTest, and 0.75 (0.64–0.86) in APRI, showing similar values between them. On the other hand, the AUC for F4 cirrhosis was 0.91 (0.84–0.98) in VTQ, 0.91 (0.84–0.97) in FibroScan, 0.82 (0.73–0.92) in FibroTest, and 0.76 (0.64–0.87) in APRI, indicating that VTQ and FibroScan were superior to serum markers (Fig. 30)²⁵.

In a multicenter study of chronic hepatitis C patients in five countries, Sporea et al. defined that measurement was reliable if the result was not “X.XX” in VTQ imaging and if the result was >60% valid and the interquartile range (IQR) was <1/3 of the measurement value in FibroScan¹⁰. They found a reliability of 98.8% for VTQ and 93.7% for FibroScan ($p=0.003$). V_s values were 1.09 ± 0.42 m/s in F0 fibrosis, 1.22 ± 0.41 m/s in F1, 1.37 ± 0.48 m/s in F2, 1.70 ± 0.59 m/s in F3, and 2.23 ± 0.71 m/s in F4, with a significant difference between adjacent stages (Fig. 31). In addition, the positive predictive value for patients with F1 or more advanced fibrosis and the negative predictive value for patients with F4 cirrhosis were as high as 95.4%, and 93.7%, respectively (Table 1). Although the diagnostic capability of FibroScan was superior to VTQ for F1 or above (AUROC, FibroScan 0.857 vs. VTQ 0.772, $p = 0.01$) and F4 (0.932 vs. 0.885, $p = 0.01$), FibroScan and VTQ had similar diagnostic capabilities for F2 or above (0.818 vs. 0.813, $p = 0.77$) and F3 or above (0.866 vs. 0.862, $p = 0.81$). Moreover, the levels of alanine aminotransferase (ALT) affected VTQ measurements as the cut-off values increased with increasing ALT values (Table 2)²⁸.

E) Limitations

Measurement may not be successful in extremely obese patients. It should be noted that liver stiffness and Vs values increase in acute liver failure and obstructive jaundice, as in FibroScan, for this phenomenon is common to all shear wave imaging (Fig. 32)^{37,38}.

It is essential to perform imaging at a sufficient depth to generate stable shear waves. However, the depth of ROI should be <8 cm, and while this would not cause any problem in the measurement of liver stiffness because the ROI is generally placed at 1–2 cm from the surface of the liver, this depth may be problematic in the assessment of liver tumors.

Although FibroScan cannot be applied to cases with ascites retention, VTQ is applicable in such cases because focused US can propagate in ascites.

VTQ fulfills the certification criteria established by both the Ministry of Health, Labour and Welfare in Japan and the FDA in USA. However, because the transmitted US waveform and the wave length are different from those of the conventional US wave, the influence of VTQ on the human body is not yet clear, and further investigation is needed for cases where safety is the highest priority. In addition, if a contrast agent is used, VTQ should be used with caution only after enough time has passed for micro bubbles and the derivatives to be excreted from the body (the Ultrasound Equipment and Safety Committee of the Japan Society of Ultrasonics in Medicine; http://www.jsum.or.jp/committee/m_and_s/acoustic_radiation.html).

The earlier version VTQ had issues such as no elasticity mapping function or the selection of only one site per measurement. Although these issues have been improved in the S3000 version, which is currently on the market under the name Virtual Touch IQ (VTIQ) and is used only for superficial imaging with a linear probe, the size of a ROI is still not adjustable and the system currently cannot be used with a convex probe. Therefore, further improvement of the system is desired.

F) Recommendations

With VTQ, it is possible to quantify shear wave propagation velocity from the B-mode image. Unlike FibroScan developed earlier, VTQ uses B-mode to effectively capture a diseased area and generates stable measurement results. VTQ also measures liver stiffness in patients with ascites retention because focused US propagates through ascites. Furthermore, because the probes can be used for B-mode imaging, the diagnosis of liver stiffness can be started immediately after routine clinical examination.

2.2.1.2. ElastPQ (Philips)

A) Introduction

Name: ElastPQ (PQ: point quantification)

Equipment: The iU22 xMATRIX ultrasound system (iU: Intelligent Ultrasound)

ElastPQ is a non-invasive diagnostic tool to measure tissue stiffness using an ARFI-based technology.

Immediately after image acquisition, the screen displays the image and measurement results, including the mean and median values and the deviations in kPa or m/s (Fig. 33).

* If measurement reliability is low, 0.00 kPa will be displayed as the result.

Elastic value E [kPa] is calculated using the equation $E = 3\rho V_s^2$ where V_s [m/s] is defined as the shear wave propagation velocity and ρ as tissue density (whose approximated value in the human body is 1).

An ROI can be placed anywhere but at a depth of < 8 cm.

B) Indication

1. Quantitative assessment of liver fibrosis in diffuse liver diseases
2. Neoplastic lesions of the liver

C) Procedures (including Tips and Tricks)

1. Perform right intercostal scanning to visualize the liver
2. Steadily place the probe with minimum compression
3. Set the ROI with a depth of < 8 cm.
4. Ask the patient to breath hold (if not possible, ask the patient to breathe as shallowly as possible)
5. Push the "Update" button for quantification
6. The use of a mean value from more than 10 measurements is recommended.

Approach the right hepatic lobe from the right intercostal space. Avoid the left hepatic lobe because the measurement is affected by cardiac movement.

Breath hold without exerting abdominal pressure.

The most appropriate ROI is the center of the image, namely, immediately below the probe, and 3–5 cm from the probe surface.

Avoid blood vessels, any necrotic areas, the boundary between organs, and areas influenced by cardiac movement (ex. left hepatic lobe).

Three frequencies (R1/RP/P1) are available. The measurement sensitivity of areas deep inside the body can be improved by using a lower frequency.

D) Results (What does the value mean?)

- Healthy liver: 4 kPa (2.5–4.7 kPa, 1–1.5 m/s)
- Mild fibrosis: 7 kPa (4.7–12.0 kPa, 1.5–2.0 m/s)
- Moderate–severe fibrosis: 12 kPa (12.0–21.0 kPa, 2.0–2.5 m/s)

- Severe fibrosis: >21 kPa (>2.5 m/s)

E) Limitations

- There is a limit to measurable depth.
- ElastPQ is affected by respiratory and body movement.
- Cardiac movement also affects the system.
- Accuracy of measurement depends on the skills of the examiner.
- Measurement accuracy is generally low at the sides of an image.
- Ribs may cast lateral acoustic shadows.

F) Recommendations

At present, the number of studies using ElastPQ is not large enough to reach a definitive conclusion. We look forward to having more study results in the near future.

2.2.2. Shear wave elastography

2.2.2.1. ShearWave™ Elastography (SWE) (Super Sonic Imagine (SSI))

A) Introduction

When tissue is dislocated posteriorly by focused US beams from the probe, the restorative force of the tissue propagates laterally, generating shear waves. A conical shear wave front is formed when US beams are transmitted continuously to tissue at different depths. All the transducers are used to transmit and receive US simultaneously, and by repeating this process at high speed, which is known as Ultrafast™ imaging, the propagation velocity of the shear wave is measured and video mapping is performed. A two-dimensional map is created when the speed of the passing shear wave is calculated based on the speed of the Doppler phase shift on a scan line. In ShearWave™ elastography (SWE), UltraFast™ imaging of the liver is performed at 3,000 frames/s.

The relationship between tissue elasticity (E) and propagation velocity of the shear wave (c) is expressed by $E = 3\rho c^2$ (ρ , tissue density). Shear waves propagate fast through hard tissue and slow through soft tissue. Tissue elasticity is calculated and based on the velocity. Measured value is expressed in kilopascals (kPa) or speed (m/s). The elastic values or velocities are color-coded, and the color-map is superimposed onto a B-mode image in real time (Fig. 34).

B) Indication

SWE has been used for the diagnosis of liver fibrosis³⁹⁻⁴² and the prognosis of liver transplant rejection and recurrent hepatitis⁴³.

Potential application of SWE to the diagnosis and localized treatment of neoplastic hepatic lesions is currently being investigated.

C) Procedures (including Tips and Tricks)

1. Use the SC6-1 convex probe and select the abdominal application
2. Display the area of interest at the center of the screen
3. Turn on the “SWE” switch
4. Adjust the size and location of the ROI
5. Push the “Freeze” button after the SWE color-map stabilizes
6. Before activating the “Q-Box” quantification tool, select and save the most appropriate frame on the system’s hard drive. The saved raw data can be used to adjust the range of a color map or to perform Q-Box quantification.
7. Adjust the range of color mapping as needed
8. Use the Q-Box tool to quantify shear wave velocity and elasticity at any location in the ROI.

Size and Depth of ROI

Size of the ROI for color mapping is adjustable up to 3×3 cm. The depth is also adjustable and can be set at any location on the frame.

Measurement results are often unreliable at a depth of >8 cm or when the ROI is placed near the edge of an image.

Imaging Tips and Tricks

- Successful SWE images can be obtained by right intercostal scanning of the right hepatic lobe. Compared with the right hepatic lobe, measurement of the left hepatic lobe is difficult because of cardiac movement. Intercostal scanning is recommended to avoid excessive compression of the liver by the probe.
- Before starting the SWE mode, clear B-mode images with no or few artifacts should be displayed.
- In the SWE mode, the movement of the probe should be kept to the minimum, and the patient needs to breath hold for a few seconds.
- The use of lower B-mode frequencies may be necessary if deep attenuation occurs.

D) Results (What does the value mean?)

SWE measures the propagation velocity of the shear wave and converts it to the Young's modulus (E) for display. The relationship between the Young's modulus (E) and shear wave velocity (c) is expressed by the equation $E=3\rho c^2$ (ρ , tissue density). Strictly speaking, the actual density of the body organ or tissue where the elasticity is being measured should be entered as ρ . However, SWE uses the density of water (i.e., 1,000 kg/m³) to calculate the Young's modulus, with the assumption that the density of tissue is close to that of water. In other words, when using the SWE quantification tool, it should be remembered that the Young's modulus is calculated based on the assumption that tissue densities are uniform. The United States Food and Drug Administration (FDA) has approved only the use of m/s as a velocity indicator; however, both kPa and m/s are displayed in other regions (Fig. 35). The maximum measurement value is 300 kPa (10 m/s).

1) Diagnosis of liver fibrosis

Bavu et al. reported that biopsy staging of liver fibrosis was correlated with the calculated values of Young's modulus (Fig. 36)³⁹. The area under the receiver operating characteristic (AUROC) for F2 or above, F3 or above, and F4 were 0.846, 0.857, and 0.940, respectively, using FibroScan, whereas SWE had overall higher values of 0.948, 0.962, and 0.968, respectively (Fig. 37)³⁹. Ferraioli et al. also reported high AUROC values of 0.92 for F2 or above, 0.98 for F3 or above, and 0.98 for F4 in fibrosis staging (Fig. 38)⁴⁰.

In addition, Bavu et al. reported that despite the different measurement values between FibroScan and SWE, the SSI values (c) became very similar to those of FibroScan (d) when shear wave spectroscopy was used to recalculate supersonic shear imaging (SSI) data under the assumption that the original measurement had been performed at 50 Hz, the shear wave frequency used in FibroScan (Fig. 39). When heterogeneity was defined as $\tau = \frac{\sigma}{E}$, it tended to increase with the progression of fibrosis from 14.24% at F0-1 to 16.63% at F2, 17.62% at F3, and 19.29% at F4 (Fig. 40)³⁹.

2) Space occupying lesion

It is possible to comparatively assess differences between a tumor and non-tumor area or between homogenous and heterogeneous parts of the tumor, and by using the Q-Box tool, tissue elasticity and

shear wave velocity at any location in the ROI can be expressed in absolute numbers (Figs. 41, 42).

E) Limitations

- Accurate subcostal scanning of the left hepatic lobe may be difficult due to cardiac movement.
- Because there is a limit to the measurable depth because of its dependency on the acoustic output[[please confirm]], measurement may not be successful for lesions located deep inside or on the surface of the liver.
- Because the maximum ROI size is 3×3 cm, one scan may not be sufficient for some lesions.
- Because of its relatively short time on the market, the number of evidence-based studies using this new technology is insufficient to establish diagnostic criteria.
- SWE is reportedly influenced by blood stasis, or congestion⁴⁴. In principle, SWE is also affected by inflammation and jaundice.

F) Recommendations

SWE quantifies the shear wave propagation velocity and displays it on a two-dimensional map. Owing to the mapping capability, velocity heterogeneity in diffuse liver disease is displayed on the map. This is particularly useful for the assessment of liver with inconsistent elasticity, as found in patients with focal fatty infiltration or Budd-Chiari syndrome.

In space occupying lesions, SWE visualizes the changes in the elasticity of the tumor and surrounding tissue, and studies are currently underway to elucidate the efficacy of SWE in the differential diagnosis of space occupying lesions of the liver and in the determination of ablation range in localized treatment, such as radiofrequency ablation therapy.

2.2.3. Transient elastography

2.2.3.1. FibroScan® (Echosens)

A) Introduction

There is a positive correlation between liver stiffness and fibrosis. To quantify liver elasticity, FibroScan® measures the propagation velocity of single-cycle shear wave generated by a probe unique to FibroScan^{45, 46}. A low-frequency elastic wave is generated by the vibration at the probe tip and is transmitted from the body surface to the liver through the skin and adipose tissue. The system uses US to track the vibration and measures the velocity. To quantify liver stiffness, the elastic value E [kPa] is calculated using the following equation, where Vs [m/s] is the shear wave propagation velocity and ρ is tissue density (the approximate density of the human body is 1).

$$E = 3\rho V_s^2$$

Measurement sites should be somewhere between 25 and 65 mm from the body surface, and numerical conversion takes place upon the imaging of at least 20 mm (Fig. 43).

B) Indication

FibroScan is indicated for patients who have or who are suspected to have chronic liver disease and require an assessment of liver fibrosis. For example, because aggressive therapy is recommended for patients with advanced fibrosis, the severity of liver fibrosis in chronic hepatitis C patients needs to be diagnosed before deciding the indication for treatment with potential side effects⁴⁶⁻⁵⁰. In addition, the rate of fibrosis progression can be estimated by performing the measurement on a regular basis⁵¹⁻⁵⁴, and the elastic values of liver tissue are an important indicator for the screening of esophageal varices⁵⁵⁻⁵⁷. FibroScan is also useful in the assessment of hepatitis B^{58, 59}, alcoholic hepatitis, non-alcoholic steatohepatitis^{60, 61}, autoimmune liver disease such as primary biliary cirrhosis and primary sclerosing cholangitis^{62, 63}, and HCV-HIV co-infection cases⁶⁴. FibroScan has also been used to evaluate the severity of portal hypertension after a liver transplant^{65, 66}. Because it is extremely minimally invasive and can be completed quickly, FibroScan will be useful for the screening of chronic liver disease in outpatients with diabetes^{67, 68}.

C) Procedures (including Tips and Tricks)

In principle, imaging should be performed while fasting because liver stiffness reportedly increases after a meal⁶⁹. With appropriate force, press the FibroScan® probe vertically against the skin, with the patient lying down with the right arm elevated to make the intercostal spaces wider. While watching the pressure indicator on the screen, adjust the compression to the chest and push the button to generate a low frequency wave. This light impacts on the liver, and the system uses US pulses to measure the velocity of the low frequency wave and calculates tissue elasticity for display (Fig. 43).

It may be necessary to confirm the location of the liver in advance using B-mode US beams because the location varies greatly among individuals. In addition, select a wide intercostal space to capture a large portion of the liver. With practice, it will be easier to determine which intercostal space is more appropriate for B-mode imaging. To avoid the adverse effects of the ribs, the probe should be pressed vertically against the thoracic wall on the axillary line and between the ribs. Errors can be

minimized if imaging is performed while breath holding⁷⁰. An error indication appears after unsuccessful measurement. Measurement should be repeated at least 10 times to obtain a median value and IQR. When the rate of successful measurements out of all measurements is <60% or when the value of IQR/median is >0.3, measurement values are of low quality and should not be used in clinical decision making.

D) Results (What does the value mean?)

Measurement values are expressed in elasticity [kPa]. The higher the value, the more difficult it is to deform the liver, indicating that fibrosis is more advanced. Although there is certain variability between studies and diseases, elasticity of ≥ 7 kPa and ≥ 12.5 –15 kPa is considered to indicate significant fibrosis and cirrhosis, respectively (Fig. 44)⁴⁵. A meta-analysis of previous studies using transient elastography, or FibroScan, have shown that the sensitivity and specificity for the diagnosis of cirrhosis were 0.87 (95% confidence interval, 0.84–0.90) and 0.91 (0.89–0.92), respectively, and those for fibrosis staging of F2–4 were 0.91 (0.81–0.96) and 0.85 (0.81–0.87), respectively (Fig. 45)⁷¹. The upper limit of measurement is 75 kPa, and although liver cirrhosis based on biopsy is generally categorized as F4, several studies have shown that there is a positive correlation between liver stiffness (elasticity) and cancer risks even if the elasticity is >15 kPa (Figs. 46, 47)^{72,73}. It should be noted that measurement values are also high when liver elasticity is increased by factors other than fibrosis, such as acute hepatitis, jaundice, and congestive liver (Figs. 50–53)^{19–22, 74, 75}.

E) Limitations

Approximately 5% of all FibroScan imaging has some problems in quantification^{76–78}. Imaging is not possible in cases in which ascites retention is near the surface of the liver being examined. In addition, measurement reproducibility decreases in fatty liver and obese cases⁷⁹. The relationship between liver elasticity and the progression of liver fibrosis reportedly varies depending on the underlying liver disease⁸⁰. Inflammation, jaundice, and congestion frequently exacerbate liver stiffness, making accurate assessment of fibrosis difficult^{21, 22, 75}. The severity of fibrosis may be underestimated in cirrhotic liver with large regenerative nodules⁸¹. In addition, measurements are difficult in severely obese individuals because of a relatively long distance between the body surface and the liver. Overseas, a probe has been developed for use with severely obese individuals and is used in clinical practice^{82, 83}.

F) Recommendations

FibroScan is the most popular and highly trusted liver elastography technique because of the large amount of validation data accumulated to date.

The system is recommended for the screening of chronic liver diseases and follow-up observations.

Depending on the existing disease conditions, measurement values may not accurately reflect the actual severity of liver fibrosis, and the system should therefore be used with the limitations described above in mind.

References

1. Matsumura T, Shiina T, Oosaka T, et al. Development of real-time tissue elastography. *MEDIX* 2004;41:30-5.
2. Tatsumi C, Kudo M, Ueshima K, et al. Noninvasive evaluation of hepatic fibrosis using serum fibrotic markers, transient elastography (FibroScan) and real-time tissue elastography. *Intervirolgy* 2008;51(Suppl 1):27-33.
3. Tatsumi C, Kudo M, Ueshima K, et al. Non-invasive evaluation of hepatic fibrosis for type C chronic hepatitis. *Intervirolgy* 2010;53:76-81.
4. Fujimoto K, Wada S, Oshita M, et al. Non-invasive evaluation of hepatic fibrosis in patients with choronic hepatitis C using elastography. *MEDIX* 2007;Suppl.:24-7.
5. Fujimoto K, Kato M, Tonomura A, et al. Non-invasive evaluation method of the liver fibrosis using real-time tissue elastograpy -usefulness of judgment liver fibrosis stage by liver fibrosis index (LF Index). *Kanzo* 2010;59:539-41.
6. Koizumi Y, Hirooka M, Kisaka Y, et al. Liver fibrosis in patients with chronic hepatitis C: noninvasive diagnosis by means of real-time tissue elastography - establishment of the method for measurement. *Radiology* 2011;258:610-7.
7. Morikawa H, Fukuda K, Kobayashi S, et al. Real-time tissue elastography as a tool for the noninvasive assessment of liver stiffness in patients with chronic hepatitis C. *J Gastroenterol* 2011;46:350-8.
8. Fujimoto K, Kato M, Kudo M, et al. Novel image analysis method using ultrasound elastography for non-invasive evaluation of hepatic fibrosis in patients with chronic hepatitis C. *Oncology* 2013;84 (supple 1):3-12.
9. Yada N, Kudo M, Morikawa H, et al. Assessment of liver fibrosis with real-time tissue elastography in chronic viral hepatitis. *Oncology* 2013;84 (suppl 1):13-20.
10. Ochi H, Hirooka M, Koizumi Y, et al. Real-time tissue elastography for evaluation of hepatic fibrosis and portal hypertension in nonalcoholic fatty liver diseases. *Hepatology* 2012;56:1271-8.
11. Hirooka M, Ochi H, Koizumi Y, et al. Splenic elasticity measured with real-time tissue elastography is a marker of portal hypertension. *Radiology* 2011;261:960-8.
12. Tonomura A, Waki K, Imura T, et al. Development of strain histogram measurement function and clinical applications in hepatic region. *MEDIX* 2011;54:37-41.
13. Saftoiu A, Gheonea DI, Ciurea T. Hue histogram analysis of real-time elastography images for noninvasive assessment of liver fibrosis. *AJR Am J Roentgenol* 2007;189:W232-3.
14. Kanamoto M, Shimada M, Ikegami T, et al. Real time elastography for noninvasive diagnosis of liver fibrosis. *J Hepatobiliary Pancreat Surg* 2009;16:463-7.
15. Ferraioli G, Lissandrin R, Filice C. Real-time tissue elastography in the assessment of liver stiffness. *Hepatology* 2012.
16. Shiina T, Maki T, Yamakawa M, et al. Mechanical model analysis for quantitative evaluation of liver fibrosis based on ultrasound tissue elasticity imaging. *Japanese Journal of Applied Physics* 2012;51:07GF11 1-8.

17. Wang J, Guo L, Shi X, et al. Real-time elastography with a novel quantitative technology for assessment of liver fibrosis in chronic hepatitis B. *Eur J Radiol* 2012;81:e31-6.
18. Friedrich-Rust M, Ong MF, Herrmann E, et al. Real-time elastography for noninvasive assessment of liver fibrosis in chronic viral hepatitis. *AJR Am J Roentgenol* 2007;188:758-64.
19. Arena U, Vizzutti F, Corti G, et al. Acute viral hepatitis increases liver stiffness values measured by transient elastography. *Hepatology* 2008;47:380-4.
20. Sagir A, Erhardt A, Schmitt M, et al. Transient elastography is unreliable for detection of cirrhosis in patients with acute liver damage. *Hepatology* 2008;47:592-5.
21. Millionig G, Reimann FM, Friedrich S, et al. Extrahepatic cholestasis increases liver stiffness (FibroScan) irrespective of fibrosis. *Hepatology* 2008;48:1718-23.
22. Colli A, Pozzoni P, Berzuini A, et al. Decompensated chronic heart failure: increased liver stiffness measured by means of transient elastography. *Radiology* 2010;257:872-8.
23. Hirooka M, Koizumi Y, Hiasa Y, et al. Hepatic elasticity in patients with ascites: evaluation with real-time tissue elastography. *AJR Am J Roentgenol* 2011;196:W766-71.
24. Shuang-Ming T, Ping Z, Ying Q, et al. Usefulness of acoustic radiation force impulse imaging in the differential diagnosis of benign and malignant liver lesions. *Acad Radiol* 2011;18:810-5.
25. Friedrich-Rust M, Wunder K, Kriener S, et al. Liver fibrosis in viral hepatitis: noninvasive assessment with acoustic radiation force impulse imaging versus transient elastography. *Radiology* 2009;252:595-604.
26. Boursier J, Isselin G, Fouchard-Hubert I, et al. Acoustic radiation force impulse: a new ultrasonographic technology for the widespread noninvasive diagnosis of liver fibrosis. *Eur J Gastroenterol Hepatol* 2010;22:1074-84.
27. Takahashi H, Ono N, Eguchi Y, et al. Evaluation of acoustic radiation force impulse elastography for fibrosis staging of chronic liver disease: a pilot study. *Liver Int* 2010;30:538-45.
28. Sporea I, Bota S, Peck-Radosavljevic M, et al. Acoustic radiation force impulse elastography for fibrosis evaluation in patients with chronic hepatitis C: an international multicenter study. *Eur J Radiol* 2012;81:4112-8.
29. Yoneda M, Suzuki K, Kato S, et al. Nonalcoholic fatty liver disease: US-based acoustic radiation force impulse elastography. *Radiology* 2010;256:640-7.
30. Palmeri ML, Wang MH, Rouze NC, et al. Noninvasive evaluation of hepatic fibrosis using acoustic radiation force-based shear stiffness in patients with nonalcoholic fatty liver disease. *J Hepatol* 2011;55:666-72.
31. Friedrich-Rust M, Romen D, Vermehren J, et al. Acoustic radiation force impulse-imaging and transient elastography for non-invasive assessment of liver fibrosis and steatosis in NAFLD. *Eur J Radiol* 2012;81:e325-31.
32. Guzman-Aroca F, Frutos-Bernal MD, Bas A, et al. Detection of non-alcoholic steatohepatitis in patients with morbid obesity before bariatric surgery: preliminary

- evaluation with acoustic radiation force impulse imaging. *Eur Radiol* 2012;22:2525-32.
33. Furuichi Y, Moriyasu F, Taira J, et al. Noninvasive diagnostic method for idiopathic portal hypertension based on measurements of liver and spleen stiffness by ARFI elastography. *J Gastroenterol* 2012.
 34. Ye XP, Ran HT, Cheng J, et al. Liver and spleen stiffness measured by acoustic radiation force impulse elastography for noninvasive assessment of liver fibrosis and esophageal varices in patients with chronic hepatitis B. *J Ultrasound Med* 2012;31:1245-53.
 35. Toshima T, Shirabe K, Takeishi K, et al. New method for assessing liver fibrosis based on acoustic radiation force impulse: a special reference to the difference between right and left liver. *J Gastroenterol* 2011;46:705-11.
 36. Ebinuma H, Saito H, Komuta M, et al. Evaluation of liver fibrosis by transient elastography using acoustic radiation force impulse: comparison with Fibroscan®. *J Gastroenterol* 2011;46:1238-48.
 37. Karlas TF, Pfrepper C, Rosendahl J, et al. Acoustic radiation force impulse (ARFI) elastography in acute liver failure: necrosis mimics cirrhosis. *Z Gastroenterol* 2011;49:443-8.
 38. Bota S, Sporea I, Sirli R, et al. Factors that influence the correlation of acoustic radiation force impulse (ARFI), elastography with liver fibrosis. *Med Ultrason* 2011;13:135-40.
 39. Bavu E, Gennisson JL, Couade M, et al. Noninvasive in vivo liver fibrosis evaluation using supersonic shear imaging: a clinical study on 113 hepatitis C virus patients. *Ultrasound Med Biol* 2011;37:1361-73.
 40. Ferraioli G, Tinelli C, Dal Bello B, et al. Accuracy of real-time shear wave elastography for assessing liver fibrosis in chronic hepatitis C: a pilot study. *Hepatology* 2012;56:2125-33.
 41. Ling W, Lu Q, Quan J, et al. Assessment of impact factors on shear wave based liver stiffness measurement. *Eur J Radiol* 2013;82:335-41.
 42. Poynard T, Munteanu M, Luckina E, et al. Liver fibrosis evaluation using real-time shear wave elastography: applicability and diagnostic performance using methods without a gold standard. *J Hepatol* 2013.
 43. Yoon JH, Lee JY, Woo HS, et al. Shear wave elastography in the evaluation of rejection or recurrent hepatitis after liver transplantation. *Eur Radiol* 2013.
 44. Wang HK, Lai YC, Tseng HS, et al. Hepatic venous congestion after living donor liver transplantation: quantitative assessment of liver stiffness using shear wave elastography--a case report. *Transplant Proc* 2012;44:814-6.
 45. Sandrin L, Fourquet B, Hasquenoph JM, et al. Transient elastography: a new noninvasive method for assessment of hepatic fibrosis. *Ultrasound Med Biol* 2003;29:1705-13.
 46. Castera L, Vergniol J, Foucher J, et al. Prospective comparison of transient elastography, Fibrotest, APRI, and liver biopsy for the assessment of fibrosis in chronic hepatitis C. *Gastroenterology* 2005;128:343-50.
 47. Colletta C, Smirne C, Fabris C, et al. Value of two noninvasive methods to detect progression of fibrosis among HCV carriers with normal aminotransferases. *Hepatology*

- 2005;42:838-45.
48. Ziol M, Handra-Luca A, Kettaneh A, et al. Noninvasive assessment of liver fibrosis by measurement of stiffness in patients with chronic hepatitis C. *Hepatology* 2005;41:48-54.
 49. Sebastiani G, Vario A, Guido M, et al. Stepwise combination algorithms of non-invasive markers to diagnose significant fibrosis in chronic hepatitis C. *Journal of Hepatology* 2006;44:686-693.
 50. Shaheen AA, Wan AF, Myers RP. FibroTest and FibroScan for the prediction of hepatitis C-related fibrosis: a systematic review of diagnostic test accuracy. *Am J Gastroenterol* 2007;102:2589-600.
 51. Castera L, Forns X, Alberti A. Non-invasive evaluation of liver fibrosis using transient elastography. *J Hepatol* 2008;48:835-47.
 52. Ogawa E, Furusyo N, Toyoda K, et al. The longitudinal quantitative assessment by transient elastography of chronic hepatitis C patients treated with pegylated interferon alpha-2b and ribavirin. *Antiviral Res* 2009;83:127-34.
 53. Ogawa E, Furusyo N, Murata M, et al. Longitudinal assessment of liver stiffness by transient elastography for chronic hepatitis B patients treated with nucleoside analog. *Hepatol Res* 2011;41:1178-88.
 54. Martinez SM, Foucher J, Combis JM, et al. Longitudinal liver stiffness assessment in patients with chronic hepatitis C undergoing antiviral therapy. *PLoS One* 2012;7:e47715.
 55. Kazemi F, Kettaneh A, N'Kontchou G, et al. Liver stiffness measurement selects patients with cirrhosis at risk of bearing large oesophageal varices. *J Hepatol* 2006;45:230-5.
 56. Vizzutti F, Arena U, Romanelli RG, et al. Liver stiffness measurement predicts severe portal hypertension in patients with HCV-related cirrhosis. *Hepatology* 2007;45:1290-7.
 57. Castera L, Pinzani M, Bosch J. Non invasive evaluation of portal hypertension using transient elastography. *J Hepatol* 2012;56:696-703.
 58. Fung J, Lai CL, But D, et al. Prevalence of fibrosis and cirrhosis in chronic hepatitis B: implications for treatment and management. *Am J Gastroenterol* 2008;103:1421-6.
 59. Wong GL, Wong VW, Choi PC, et al. Evaluation of alanine transaminase and hepatitis B virus DNA to predict liver cirrhosis in hepatitis B e antigen-negative chronic hepatitis B using transient elastography. *Am J Gastroenterol* 2008;103:3071-81.
 60. Foucher J, Chanteloup E, Vergniol J, et al. Diagnosis of cirrhosis by transient elastography (FibroScan): a prospective study. *Gut* 2006;55:403-8.
 61. Nahon P, Kettaneh A, Tengher-Barna I, et al. Assessment of liver fibrosis using transient elastography in patients with alcoholic liver disease. *J Hepatol* 2008;49:1062-8.
 62. Corpechot C, El Naggar A, Poujol-Robert A, et al. Assessment of biliary fibrosis by transient elastography in patients with PBC and PSC. *Hepatology* 2006;43:1118-24.
 63. Gomez-Dominguez E, Mendoza J, Garcia-Buey L, et al. Transient elastography to assess hepatic fibrosis in primary biliary cirrhosis. *Aliment Pharmacol Ther* 2008;27:441-7.
 64. de Ledinghen V, Douvin C, Kettaneh A, et al. Diagnosis of hepatic fibrosis and cirrhosis by transient elastography in HIV/hepatitis C virus-coinfected patients. *J Acquir Immune*

- Defic Syndr 2006;41:175-9.
65. Carrion JA, Navasa M, Bosch J, et al. Transient elastography for diagnosis of advanced fibrosis and portal hypertension in patients with hepatitis C recurrence after liver transplantation. *Liver Transpl* 2006;12:1791-8.
 66. Carrion JA, Torres F, Crespo G, et al. Liver stiffness identifies two different patterns of fibrosis progression in patients with hepatitis C virus recurrence after liver transplantation. *Hepatology* 2010;51:23-34.
 67. Roulot D, Czernichow S, Le Clesiau H, et al. Liver stiffness values in apparently healthy subjects: influence of gender and metabolic syndrome. *J Hepatol* 2008;48:606-13.
 68. Casey SP, Kemp WW, McLean CA, et al. A prospective evaluation of the role of transient elastography for the detection of hepatic fibrosis in type 2 diabetes without overt liver disease. *Scand J Gastroenterol* 2012;47:836-41.
 69. Mederacke I, Wursthorn K, Kirschner J, et al. Food intake increases liver stiffness in patients with chronic or resolved hepatitis C virus infection. *Liver Int* 2009;29:1500-6.
 70. Boursier J, Konate A, Gorea G, et al. Reproducibility of liver stiffness measurement by ultrasonographic elastometry. *Clin Gastroenterol Hepatol* 2008;6:1263-9.
 71. Talwalkar JA, Kurtz DM, Schoenleber SJ, et al. Ultrasound-based transient elastography for the detection of hepatic fibrosis: systematic review and meta-analysis. *Clin Gastroenterol Hepatol* 2007;5:1214-20.
 72. Masuzaki R, Tateishi R, Yoshida H, et al. Prospective risk assessment for hepatocellular carcinoma development in patients with chronic hepatitis C by transient elastography. *Hepatology* 2009;49:1954-61.
 73. Jung KS, Kim SU, Ahn SH, et al. Risk assessment of hepatitis B virus-related hepatocellular carcinoma development using liver stiffness measurement (FibroScan). *Hepatology* 2011;53:885-94.
 74. Coco B, Oliveri F, Maina AM, et al. Transient elastography: a new surrogate marker of liver fibrosis influenced by major changes of transaminases. *J Viral Hepat* 2007;14:360-9.
 75. Millonig G, Friedrich S, Adolf S, et al. Liver stiffness is directly influenced by central venous pressure. *J Hepatol* 2010;52:206-10.
 76. Foucher J, Castera L, Bernard PH, et al. Prevalence and factors associated with failure of liver stiffness measurement using FibroScan in a prospective study of 2114 examinations. *Eur J Gastroenterol Hepatol* 2006;18:411-2.
 77. Kettaneh A, Marcellin P, Douvin C, et al. Features associated with success rate and performance of FibroScan measurements for the diagnosis of cirrhosis in HCV patients: a prospective study of 935 patients. *J Hepatol* 2007;46:628-34.
 78. Castera L, Foucher J, Bernard PH, et al. Pitfalls of liver stiffness measurement: a 5-year prospective study of 13,369 examinations. *Hepatology* 2010;51:828-35.
 79. Fraquelli M, Rigamonti C, Casazza G, et al. Reproducibility of transient elastography in the evaluation of liver fibrosis in patients with chronic liver disease. *Gut* 2007;56:968-73.
 80. Friedrich-Rust M, Ong MF, Martens S, et al. Performance of transient elastography for the

- staging of liver fibrosis: a meta-analysis. *Gastroenterology* 2008;134:960-74.
81. Ganne-Carrie N, Ziol M, de Ledinghen V, et al. Accuracy of liver stiffness measurement for the diagnosis of cirrhosis in patients with chronic liver diseases. *Hepatology* 2006;44:1511-7.
 82. Myers RP, Pomier-Layrargues G, Kirsch R, et al. Discordance in fibrosis staging between liver biopsy and transient elastography using the FibroScan XL probe. *J Hepatol* 2012;56:564-70.
 83. Wong VW, Vergniol J, Wong GL, et al. Liver stiffness measurement using XL probe in patients with nonalcoholic fatty liver disease. *Am J Gastroenterol* 2012;107:1862-71.

table and figure legends

Table 1.

Diagnostic value of VTQ for liver fibrosis²⁸.

Table 2.

Comparison of mean liver fibrosis values assessed by ARFI (m/s) for the same stage of liver fibrosis, according to the ALT level. Significantly high Vs values in patients with high ALT levels²⁸.

Figure 1.

Principle of RTE.

Figure 2.

RTE imaging. Left, superimposition of RTE and B-mode images; right, B-mode image. The measurement tool calculates feature values and strain ratio.

Figure 3.

RTE image artifacts. Multiple reflection echo (a), large blood vessel (b), acoustic shadow (c), and poor ultrasound penetration (d) are major artifacts of RTE. For RTE, these artifacts should be avoided¹².

Figure 4.

Electrocardiogram and strain graph in liver RTE. Good RTE images may be obtained in the end of left ventricular diastole in electrocardiographic gating (arrow) (a) or at the largest downward wave on a strain graph (arrow) (b). Double-headed red arrow corresponds to one heartbeat.

Figure 5.

RTE images reflecting different stages of liver fibrosis in chronic viral hepatitis C patients. With fibrosis associated to progress, strain elastogram increases color variation between relatively low strain regions and generates a patched image pattern. F1 stage (a), F2 stage (b), F3 stage (c), F4 stage (d)⁹.

Figure 6.

Liver Elasticity Score. Liver Elasticity Scores is obtained by visual assessment of low strain areas (blue area) on RTE images. Score 1: The entire colored area of the ROI is distorted (the entire colored area is shown as relatively uniform light green). Score 2: Partially mottled blue regions are shown in the light green colored area. Score 3: Light green and blue are mixed in the colored area (almost a fifty-fifty mix). Score 4: Most of the colored area is shown as blue⁴.

Figure 7.

Relationship between Liver Elasticity Score and liver fibrosis stage. Statistical analysis for comparison of fibrosis stages of patients with chronic hepatitis C revealed that Liver Elasticity Score was significantly higher with progression of fibrosis stage⁴.

Figure 8.

Correlation between Liver Elasticity Score and type IV collagen 7S. In patients with chronic hepatitis C, type IV Collagen 7S showed a significant correlation with Liver Elasticity Score⁴.

Figure 9.

Inverse correlation between MEAN values of RTE and liver stiffness measured by FibroScan. There was a negative correlation between liver stiffness and MEAN values of RTE ($r = -0.587$, $p < 0.05$)².

Figure 10.

Relationships between the stages of liver fibrosis and four RTE feature values (MEAN, SD, %AREA, and COMP). Box plots of each feature value corresponding to fibrosis stages F1–4 and the healthy volunteer group (HV). a MEAN, b SD, c 5AREA, and d COMP. HV, $n = 10$. F1–4, $n = 95$. * $p < 0.01$, and ** $p < 0.05$ ⁷.

Figure 11.

Relationships between liver stiffness and four RTE feature values (MEAN, SD, %AREA, and COMP). a MEAN was negatively correlated with liver stiffness (kPa) ($p < 0.01$). Correlation coefficient was -0.585 . b SD was significantly correlated with liver stiffness (kPa) ($p < 0.01$). Correlation coefficient was 0.425 . c %AREA was significantly correlated with liver stiffness (kPa) ($p < 0.01$). Correlation coefficient was 0.590 . d COMP was significantly correlated with liver stiffness (kPa) ($p < 0.01$). Correlation coefficient was 0.532 ($n = 96$). a.u. arbitrary units⁷.

Figure 12.

Relationship between the stages of liver fibrosis and LF Index. FibroIndex for each fibrosis stage; many outliers were present. * $p < 0.05$, ** $p < 0.001$, comparing between each fibrosis stage. LFI, Liver Fibrosis Index⁹.

Figure 13.

ROC (Receiver Operating Characteristic) curve of the LFI, platelet count, AST/ALT ratio, APRI, and FibroIndex for predicting F2 stage or higher fibrosis (F0–F1 vs. F2–F4). b ROC of predicting F3 stage or higher fibrosis. c ROC of predicting stage F4 fibrosis⁹.

Figure 14.

Relationship between liver fibrosis and the elasticity index in patients with chronic hepatitis B. Small circles represent outliers. There was a significant correlation between the elasticity index and liver

fibrosis ($p < 0.001$)¹⁷.

Figure 15.

Measurement of elastic ratio. The elasticity of the hepatic vein was used as the reference because the elasticity of the veins does not change over time, since they do not undergo transformations with disease, such as arteriosclerosis, and it also does not increase or decrease even when liver parenchyma becomes stiffer. Thus, small vessels with a diameter of 3 mm in the liver were used as the standard for computing the elasticity ratio, and the ROI was set as large as possible (usually 0.3×0.5 cm). The ROI in the liver parenchyma was placed 1 cm from the liver surface and was 2×1 cm in size⁶.

Figure 16.

Relationship between elastic ratio and liver fibrosis in patients with chronic hepatitis C⁶.

Figure 17.

Correlation of elastic ratios calculated by two examiners⁶.

Figure 18.

Relationship between elastic ratios and liver fibrosis or NAS in patients with NAFLD. (A) Hepatic elastic ratio for each NAFLD fibrosis stage. F1 versus F2 was not significantly different ($P = 0.717$), whereas all other combinations were significantly different. (B) Hepatic elastic ratio for each NAS. The median elastic ratios with NAS more than 5 were significantly high ($P = 0.0016$)¹⁰.

Figure 19.

Elasticity score and Elasticity-Laboratory Combination Score (with the addition of platelet counts and GGT)¹⁸.

Figure 20.

Relationship between histological grading of liver fibrosis in biopsy and RTE feature values. These graphs shows the comparison between grades and the 9 image features for evaluating the effect of inflammation on RTE image. None of the 9 image features have a correlation with grades, and Liver Activity Index (LAI), which was calculated by multiple regression analysis similar to LFI, also did not correlate with grades ($r = 0.30$)⁸.

Figure 21.

RTE image before and after the injection of artificial ascites. A, Tissue elastographic image before injection for artificial ascites shows elastic ratio of 2.79. B, B-mode ultrasound image shows layer of artificial ascites (asterisk). C, Tissue elastographic image shows elastic ratio of 2.80 in presence of ascites (asterisk)²³.

Figure 22.

eSie Touch Elasticity Imaging of metastatic liver cancer. Color-mapping (a) and grayscale display (b). Left, B-mode imaging; right, eSie Touch Elasticity Imaging superimposed on the B-mode image. Tumor appearing relatively stiff compared with the surrounding non-tumor area. SF, soft; HD, hard.

Figure 23.

Strain ratio. Left, B-mode imaging; right, eSie Touch Elasticity Imaging superimposed on the B-mode image. Strain ratio is the ratio of elasticity indexes between ROI1 and ROI2, calculated as $ROI1 / ROI2$.

Figure 24.

Representative image display of Direct Strain Elastography (GE). Left, B-mode image; right, elastographic image superimposed on the B-mode image. Quality can be monitored by bar graph and line graph.

Figure 25.

Diagnostic imaging of diffuse liver disease with Elastography (Toshiba). Strain can be quantitated by two methods, comparison with kidney (a), and strain distribution in the liver (b).

Figure 26.

Correlation between liver fibrosis and strain. There was a significant correlation between liver fibrosis and strain distribution map (provided by Dr. Koji Yamamoto, Saiseikai Matsusaka General Hospital).

Figure 27.

Assessment of stiffness of metastatic liver tumor with VTI. Left, B-mode image; right, VTI. Compared with the non-tumor area, strain of metastatic liver tumor is relatively hard (black). SF, soft; HD, hard.

Figure 28.

VTQ display panel. V_s is 1.3m/s, depth of ROI is 2.8cm.

Figure 29.

Diagnostic value of VTQ for liver fibrosis at the right hepatic lobe and left hepatic lobe. (a) ROC with VTQ at right hepatic lobe for diagnosing liver fibrosis grade $F \geq 1$ (thin black line, ROC = 0.81), $F \geq 2$ (bold black line, 0.81), $F \geq 3$ (dashed line, 0.85) and $F = 4$ (dotted line, 0.87) are shown. (b) ROC with VTQ at left hepatic lobe for diagnosing liver fibrosis grade $F \geq 1$ (thin black line, 0.69), $F \geq 2$ (bold black line, 0.71), $F \geq 3$ (dashed line, 0.76) and $F = 4$ (dotted line, 0.86) are shown. Diagnostic values of liver fibrosis with VTQ at right hepatic lobe are higher than at left hepatic lobe³⁵.

Figure 30.

ROC curves for F2 fibrosis or above (a) and F4 cirrhosis (b) in VTQ (ARFI imaging), FibroScan (transient elastography)²⁵.

Figure 31.

Relationship between fibrosis stages based on METAVIR score and liver stiffness based on VTQ results²⁸.

Figure 32.

Decrease in VTQ measurement values along with the recovery of acute liver failure³⁷

Figure 33.

Quantification of liver stiffness with ElastPQ. The velocity of shear wave is 1.14 m/s, and the velocity is converted into elasticity (3.91 kPa) using the equation described in the text.

Figure 34.

SWE in phantom. It is possible to measure and display the propagation velocity of the shear waves and tissue elasticity within an arbitrary ROI (Q-Box). Other information such as the minimum, maximum and standard deviations of elastic values as well as the size of the Q-Box are displayed on the same screen.

Figure 35.

SWE in healthy liver. The system measures the propagation velocity of the shear wave per pixel to display a color map (upper panel), and the velocity is converted into elasticity (lower panel) using the equation described in the text. Shown here, the mean shear wave velocity is 1.2 m/s, and the elasticity after conversion is 4.3 kPa.

Figure 36.

Box and whisker plots of (a) SWE (supersonic shear imaging (SSI)) and (b) FibroScan values in biopsy staging of liver fibrosis³⁹.

Figure 37.

ROC curves for SWE (solid line) and FibroScan (FS) (dashed line) for different fibrosis thresholds: (a) F0-F1 vs. F2-F4 ($p = 0.005$), (b) F0-F2 vs. F3-F4 ($p = 0.001$) and (c) F0-F3 vs. F4 ($p = 0.154$)³⁹.

Figure 38.

Comparison between SWE and FibroScan (TE) of ROC curves for the diagnosis of fibrosis in chronic hepatitis C patients. (A) F0-F1 versus F2- F4 ($\geq F2$), (B) F0-F2 versus F3-F4 ($\geq F3$), and (C) F0-F3 versus F4 ($F = 4$). In parentheses, 95% confidence intervals are shown. p values of differences between AUROCs are given⁴⁰.

Figure 39.

Correlation between SSI and FibroScan. (a) Scatter plot between liver stiffness distributions

(normalized by log transformation) assessed by FS and SWE (SSI) technique. (b) Bland-Altman plot between the SWE (SSI) measurement and the FS measurement. (c) Scatter plot between liver stiffness distributions (normalized by log transformation) assessed by FS and SWE (SSI) technique extracted from fit at 50 Hz. (d) Bland-Altman plot between the SWE (SSI) measurements fitted at 50 Hz and the FS measurement³⁹.

Figure 40.

Comparison between liver heterogeneity and fibrosis³⁹.

Figure 41.

SWE image of liver cancer. The image shows stiffness distribution in the tumor and surrounding tissue. The tumor has a low elasticity of 12 kPa at the center and much lower elasticity at the margin, compared to 30 kPa in the non-tumor area which is equivalent to the stiffness of cirrhosis.

Figure 42.

Typical SWE image of cavernous hemangioma. The tumor has high elasticity of 42 kPa at the center and it appears the hard mass is surrounded by soft liver tissue of 5.5 kPa. It is clear that the hemangioma has increased viscoelasticity.

Figure 43.

The principle of FibroScan[®]. (a) An ultrasonic probe and a shear wave generator. (b) The propagation velocity of a 20-ms shear wave is measured using 4000-Hz US. (c) The shear wave propagation velocity is equivalent to Vs. (d) Scanning is performed from the right lateral intercostal space⁴⁵.

Figure 44.

Relationship between histologic liver fibrosis staging in biopsy and liver elasticity⁴⁵.

Figure 45.

Meta-analysis of nine studies on the diagnosis of liver fibrosis. The sensitivity (a) and specificity (b) for the diagnosis of cirrhosis, and sensitivity (c) and specificity (d) for the diagnosis of F2-4 fibrosis⁷¹.

Figure 46.

Cumulative incidence of HCC development stratified based on LSM (N = 866). LSM, liver stiffness measurement⁷².

Figure 47.

Cumulative incidence rates of HCC based on stratified LSM (Kaplan-Meier plot). The cumulative incidence rates increased significantly in association with higher LSM (log-rank test, $P < 0.001$)⁷³.

Figure 48.

Transition in the levels of alanine aminotransferase (ALT), bilirubin, and liver stiffness in patients with drug-induced liver injury caused by nitrofurantoin²⁰.

Figure 49.

Relationship between liver stiffness and the level of transaminase in patients with acute viral hepatitis¹⁹.

Figure 50.

Transition in the levels of bilirubin and liver stiffness in patients with obstructive jaundice²¹.

Figure 51.

Comparison of liver stiffness between patients with acute decompensated heart failure (ADHF) and controls. Liver stiffness can be improved in ADHF patients. LS, liver stiffness²².

Table 1

Fibrosis	Cut-off (m/s)	AUROC	Se (%)	Sp (%)	Positive predictive value – PPV (%)	Negative predictive value – NPV (%)	Accuracy (%)
$F \geq 1$	>1.19	0.779	69.9	80	95.4	16	70.4
$F \geq 2$	>1.33	0.792	69.1	79.8	87.3	56.1	72.6
$F \geq 3$	>1.43	0.829	74.8	81.5	76.3	79.8	78.2
$F = 4$	>1.55	0.842	84.3	76.3	53.1	93.7	77.9

A *p*-value < 0.05 was regarded as significant.

Table 2

Fibrosis	ALT \leq ULN* (n = 394)	ALT = 1.1 – 3 \times ULN# (n = 376)	ALT > 3 \times ULN α (n = 94)	p
F0-1	1.10 \pm 0.35 (n = 156)	1.23 \pm 0.26 (n = 101)	1.42 \pm 0.49 (n = 16)	*#: 0.003 * α : 0.01 # α : 0.18
F2-3	1.40 \pm 0.49 (n = 160)	1.63 \pm 0.63 (n = 175)	1.61 \pm 0.47 (n = 43)	*#: 0.002 * α : 0.002 # α : 0.36
F4	2.07 \pm 0.76 (n = 78)	2.31 \pm 0.64 (n = 100)	2.45 \pm 0.63 (n = 35)	*#: 0.02 * α : 0.006 # α : 0.13

A p-value <0.05 was regarded as significant.

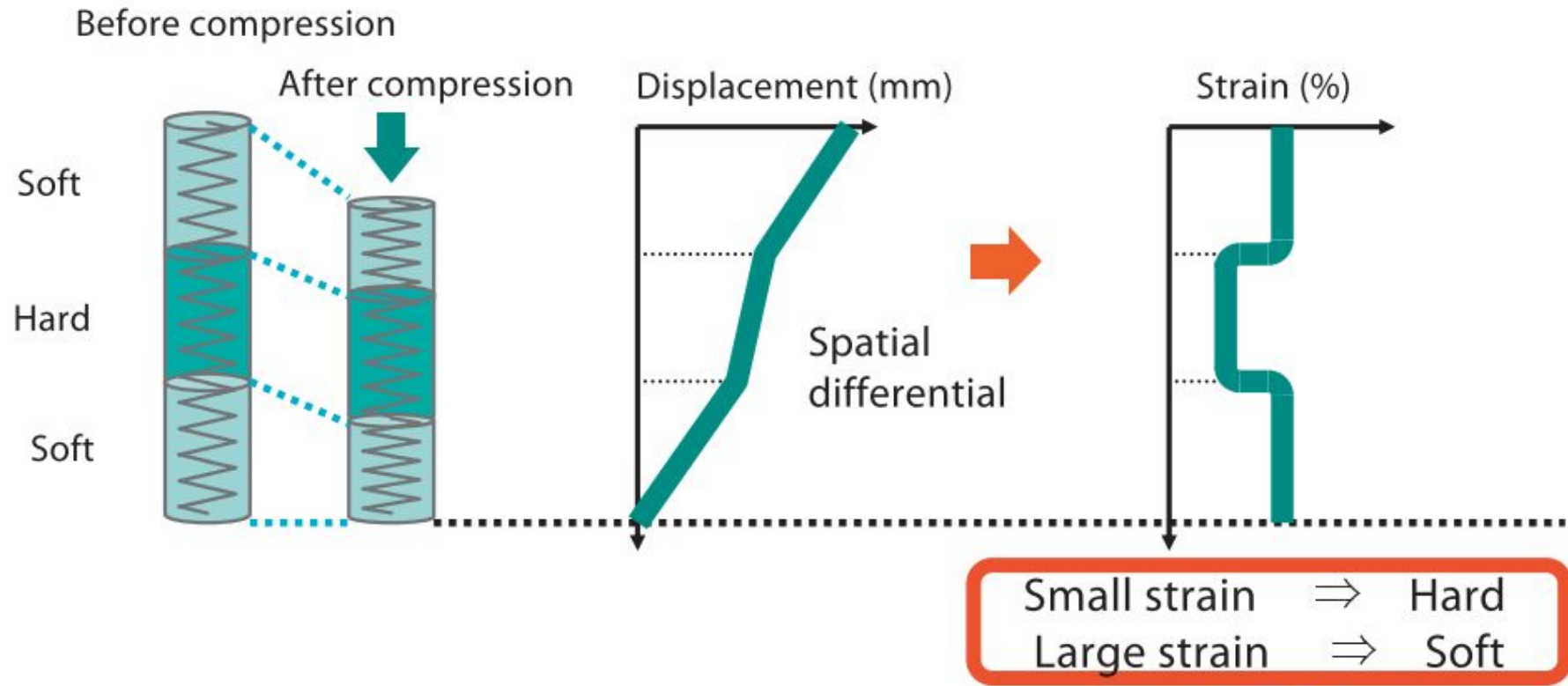
*Patients with ALT < ULN.

#Patients with ALT = 1.1 – 3 \times ULN.

α Patients with ALT > 3 \times ULN.

Fig.1

a



b

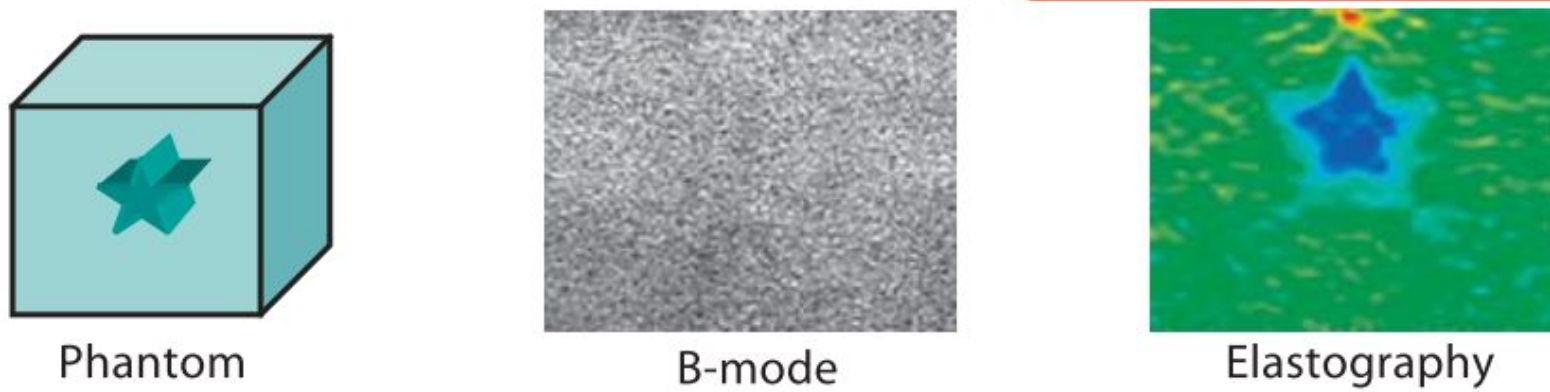


Fig.2

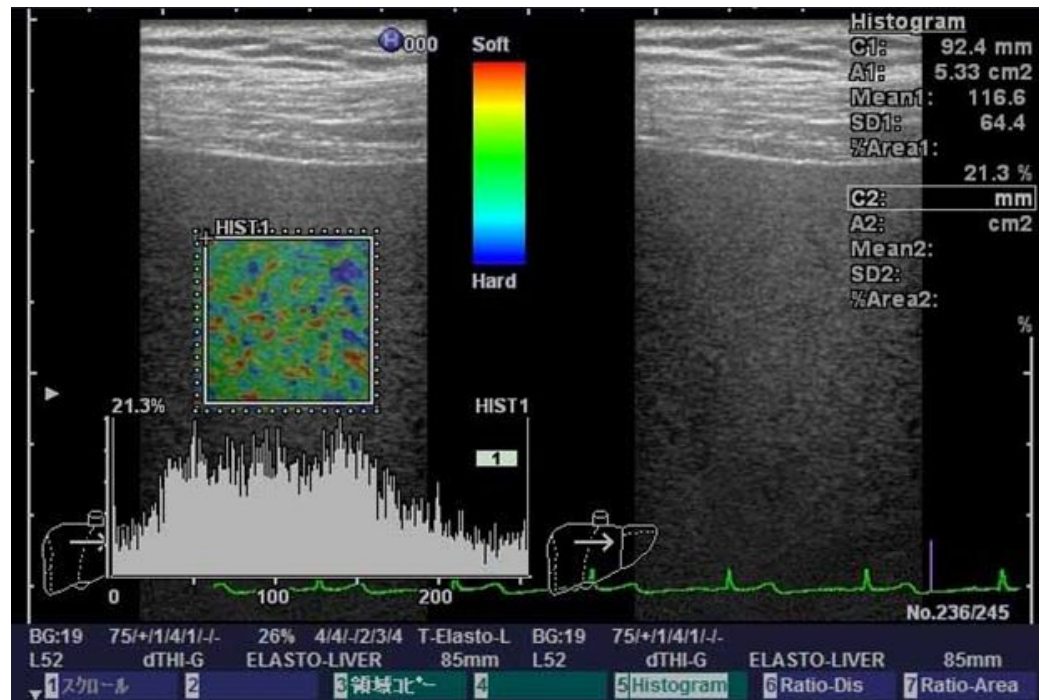


Fig.3

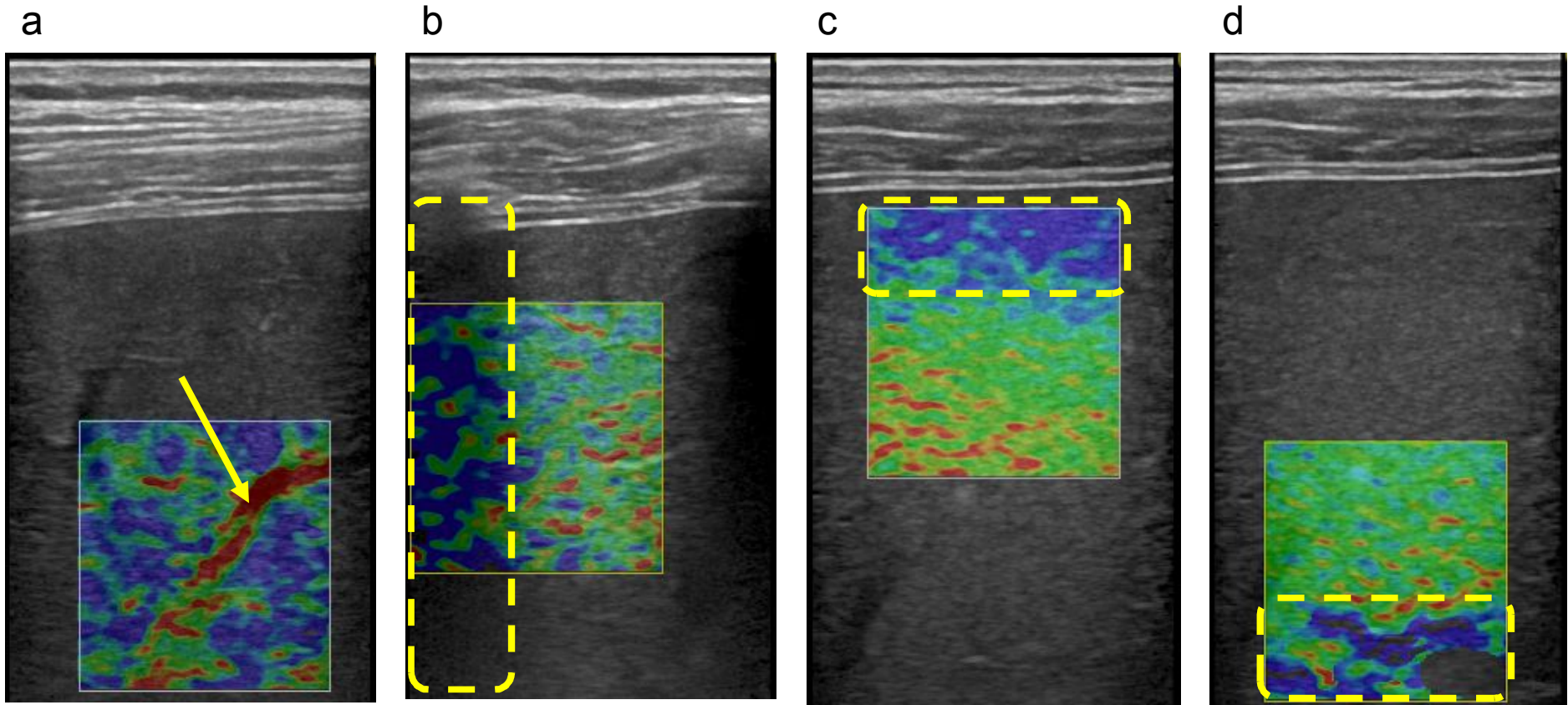


Fig.4

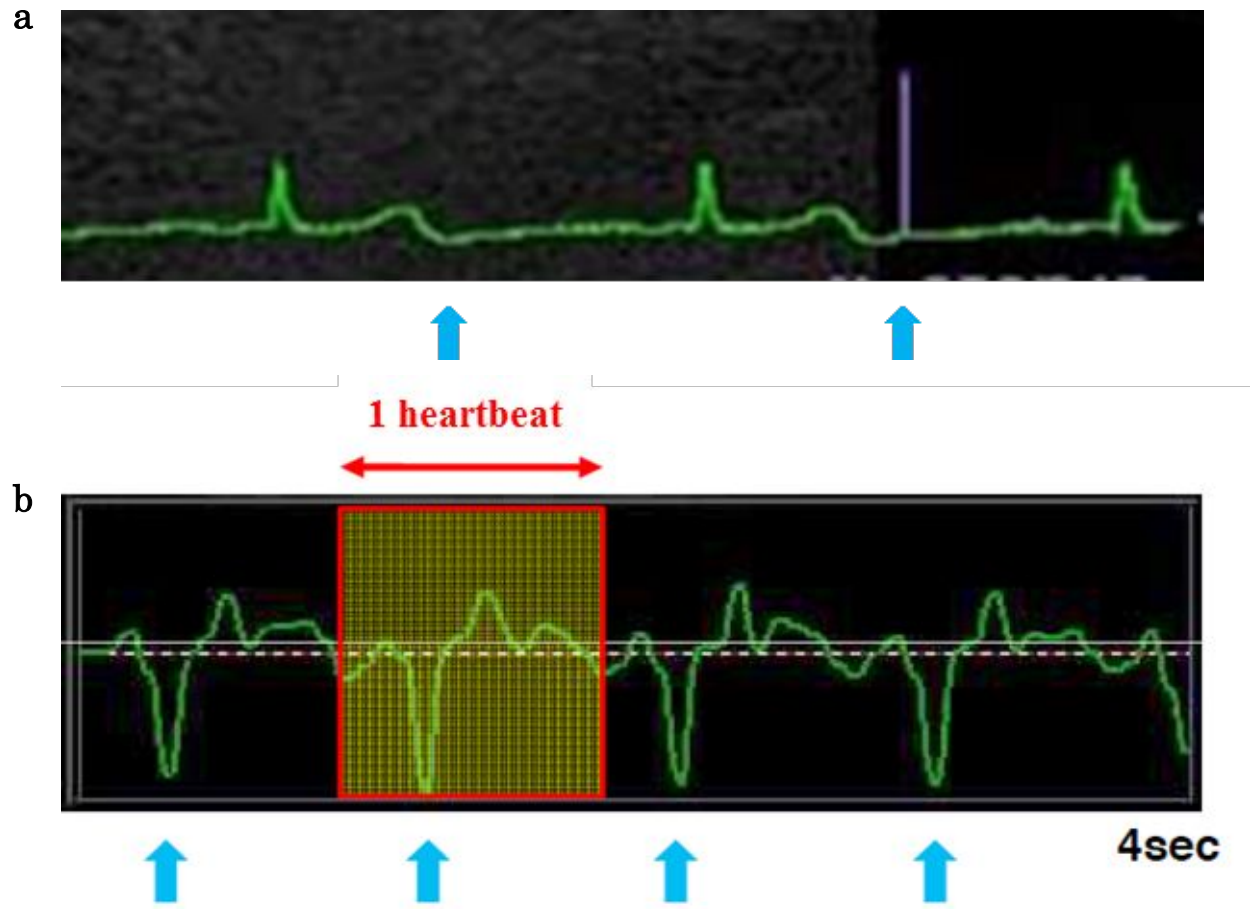


Fig.5

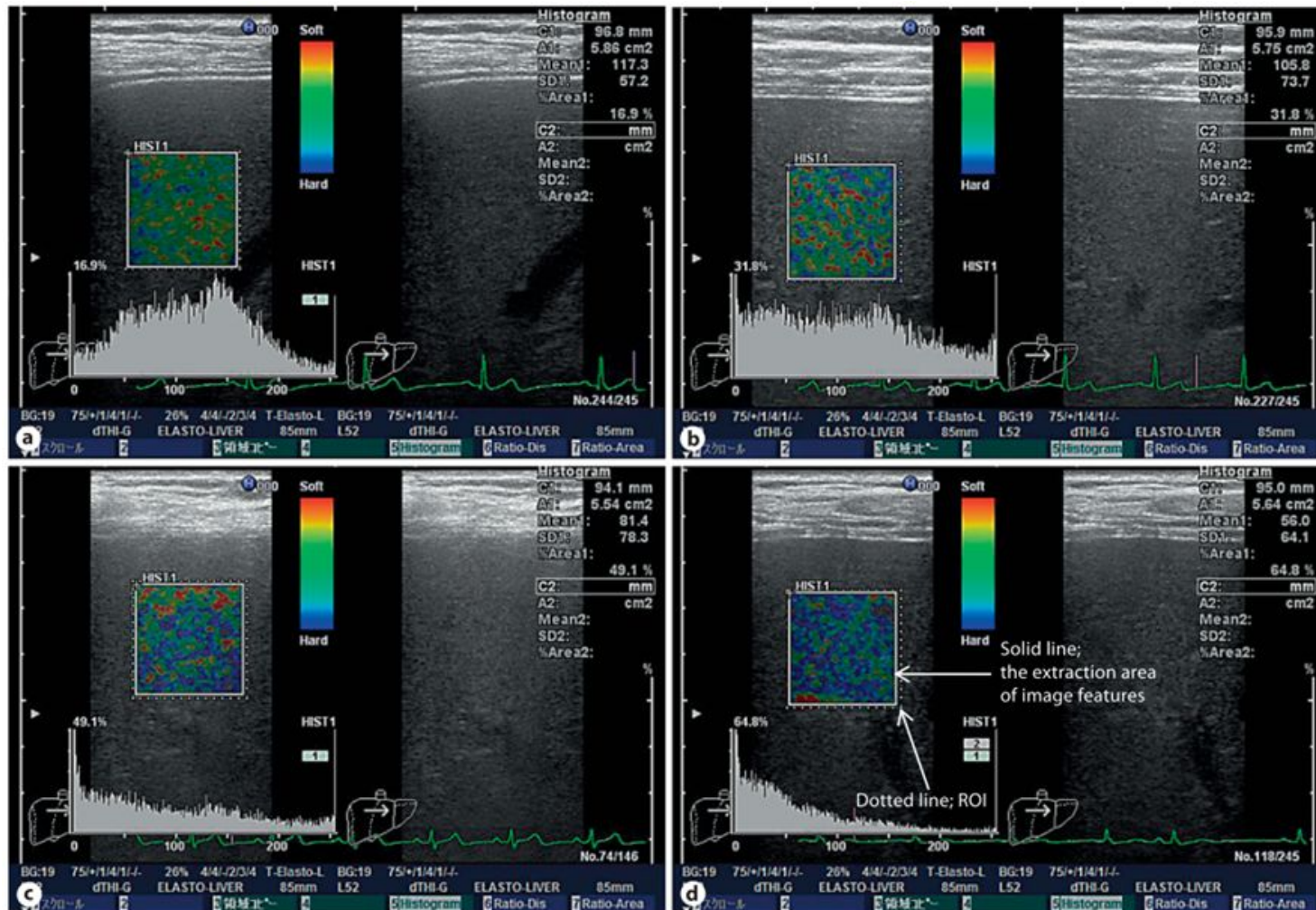


Fig.6

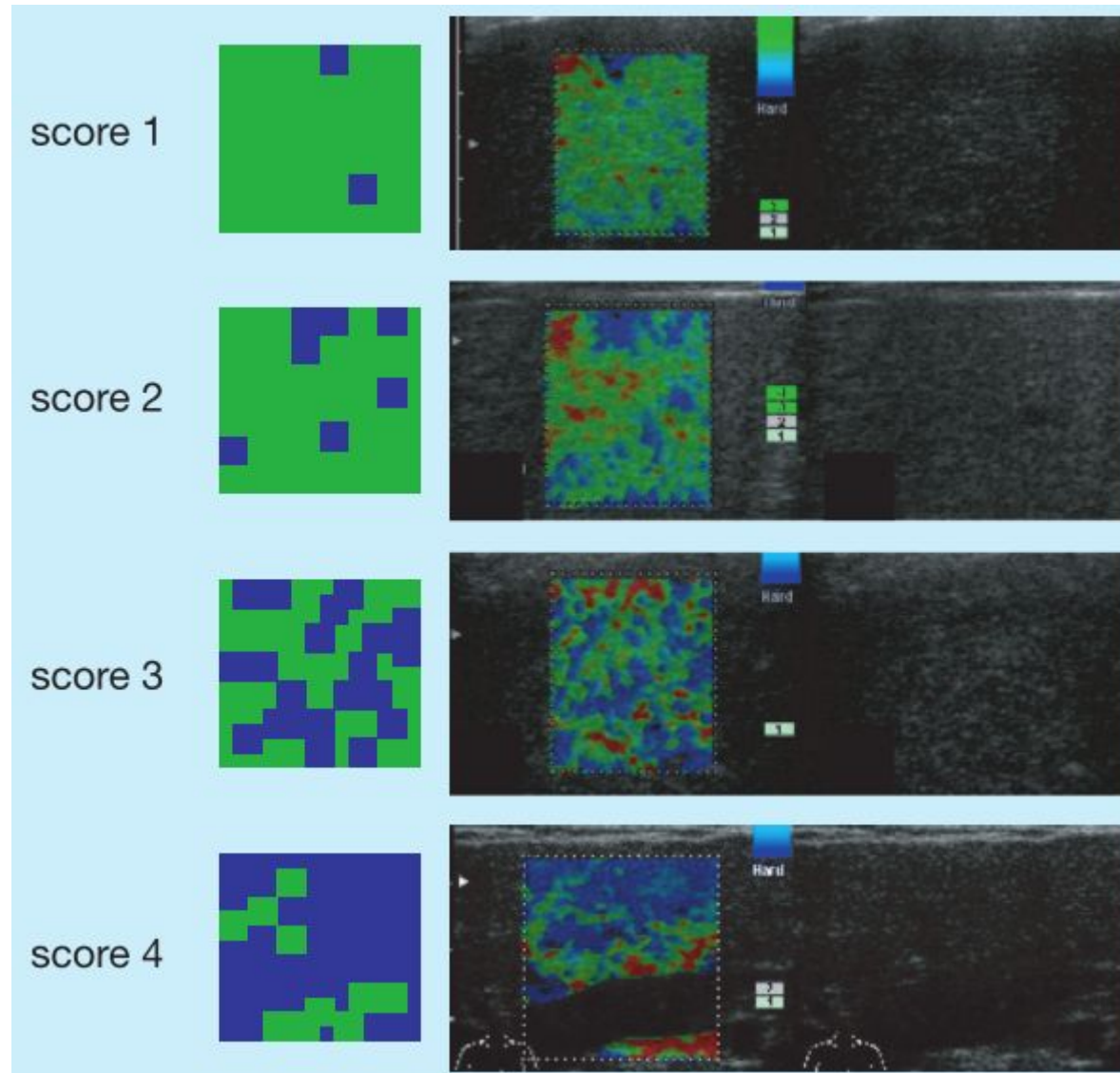


Fig.7

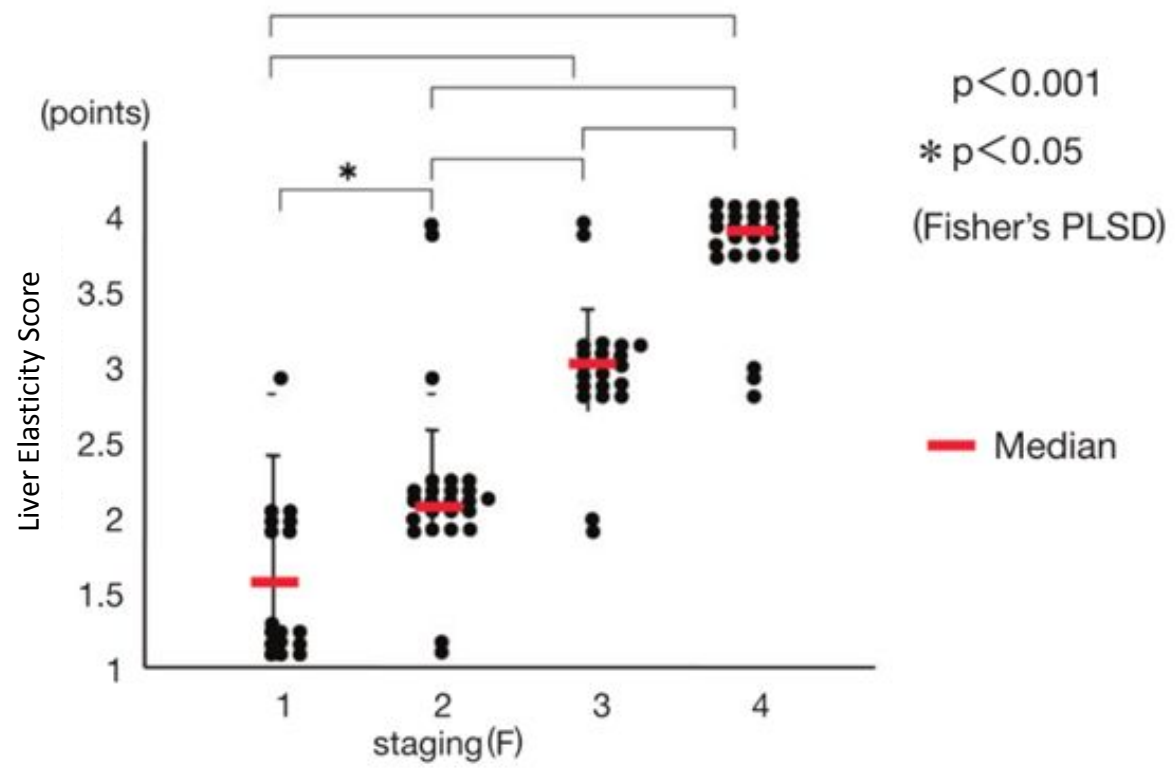


Fig.8

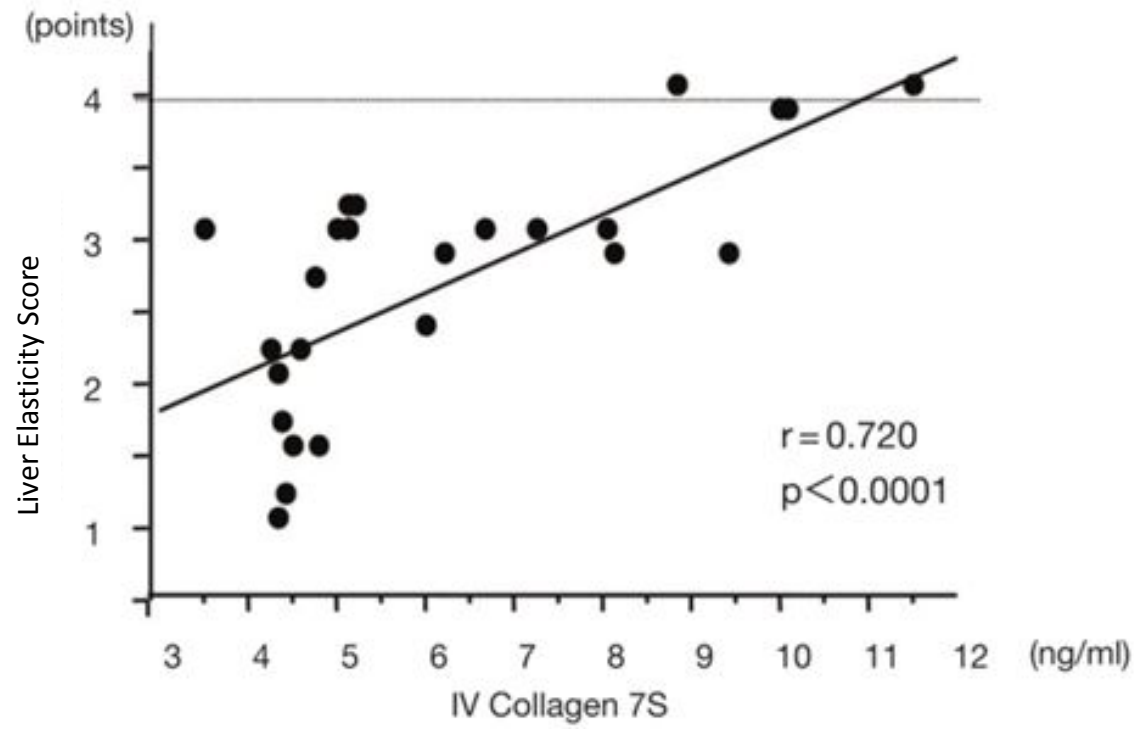


Fig.9

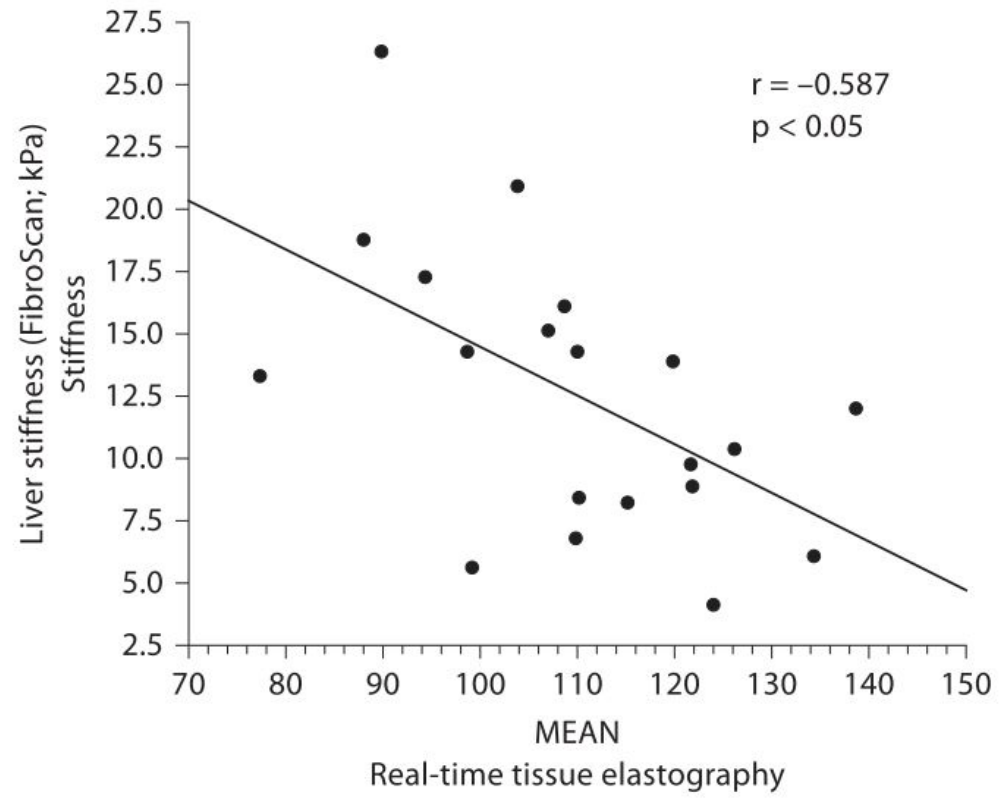


Fig.10

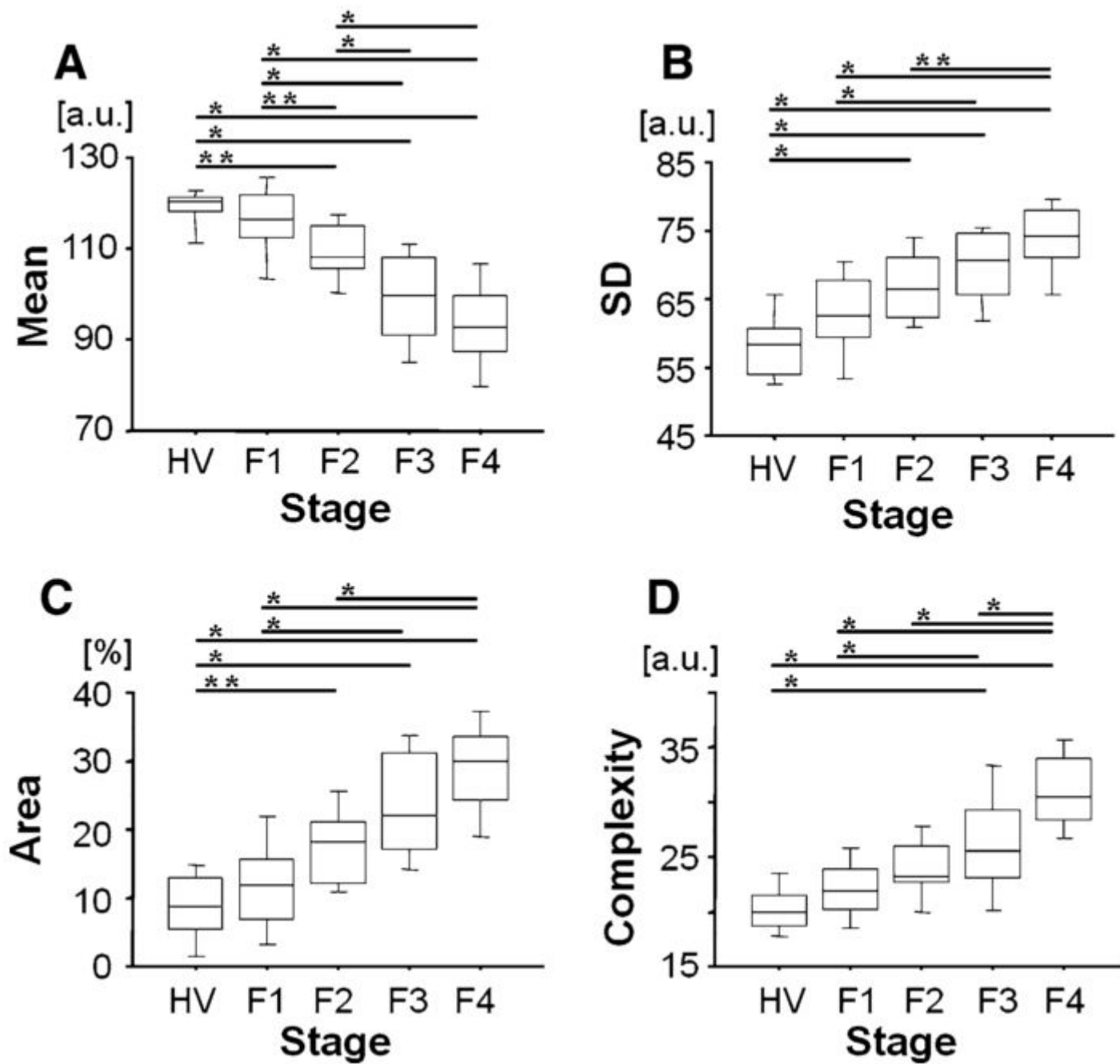


Fig.11

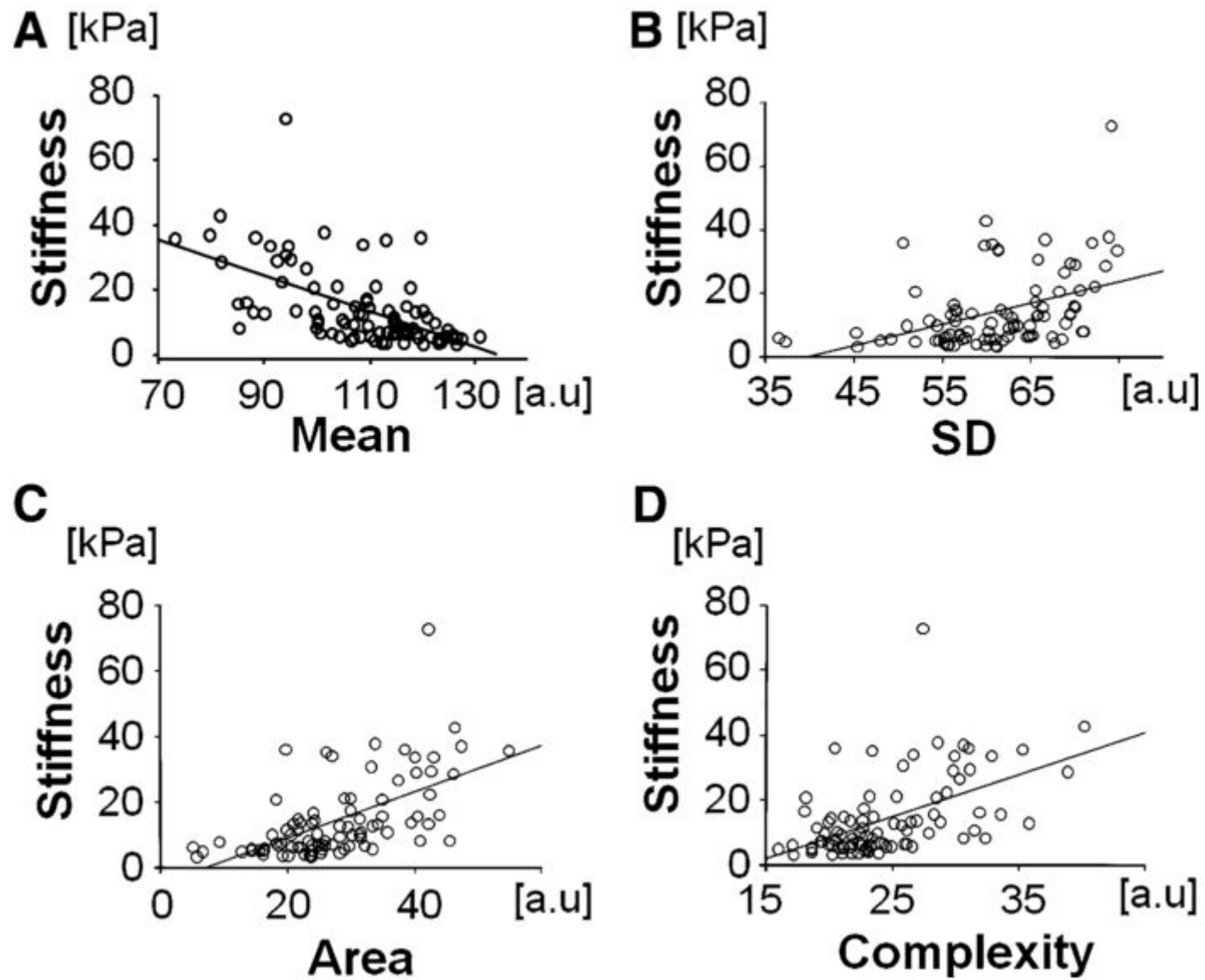


Fig.12

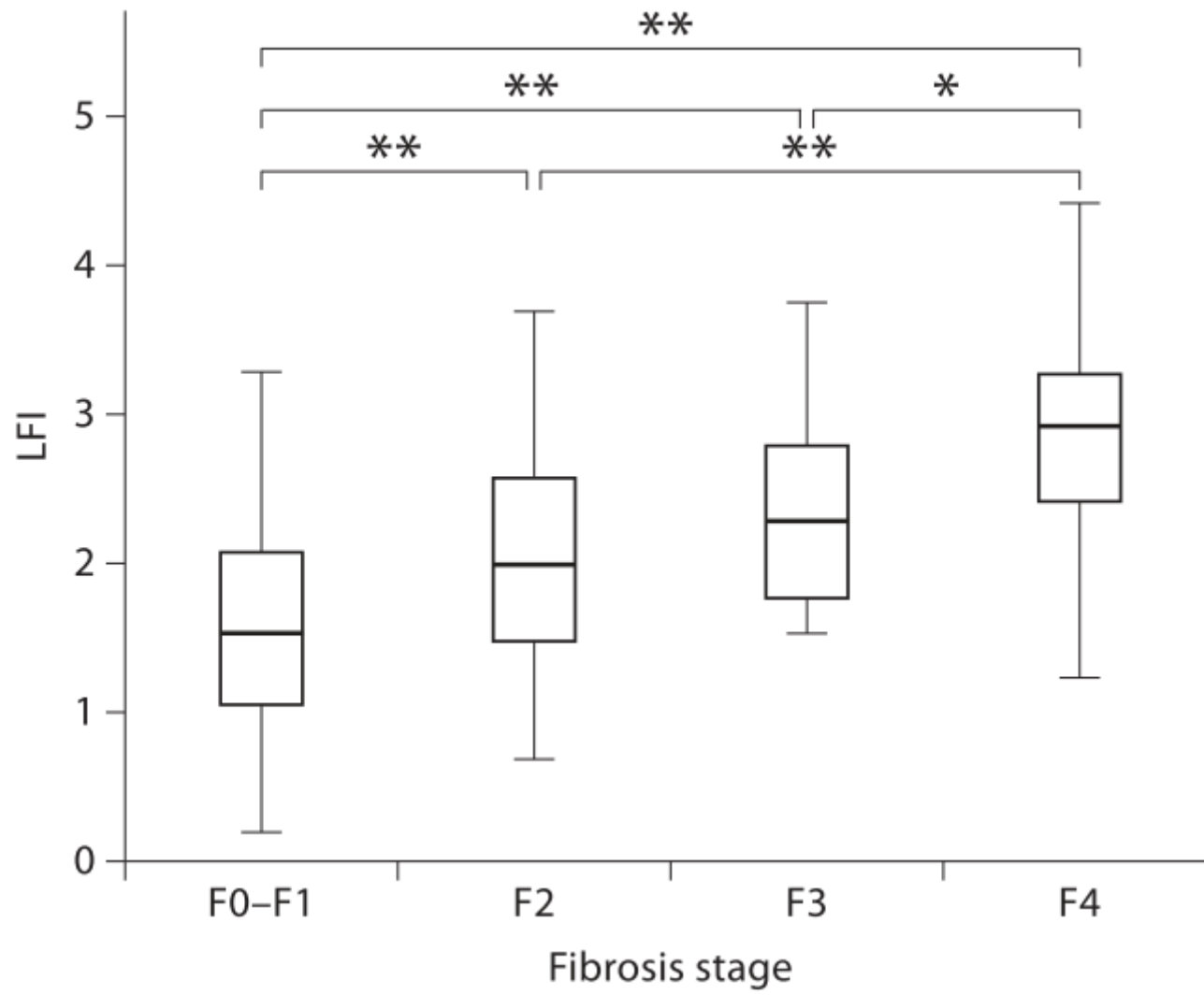


Fig.13

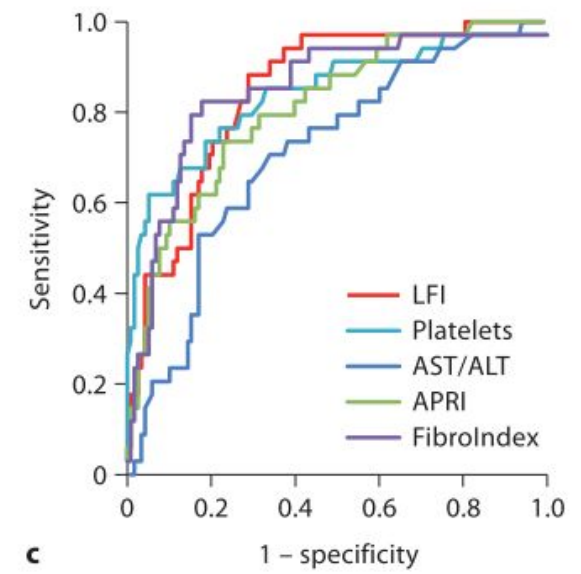
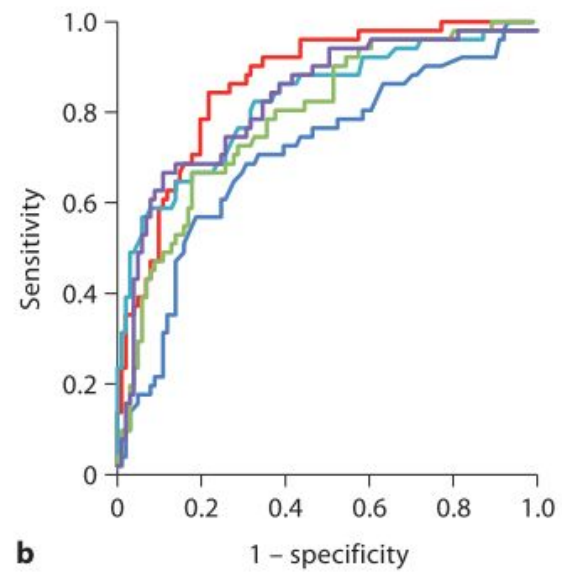
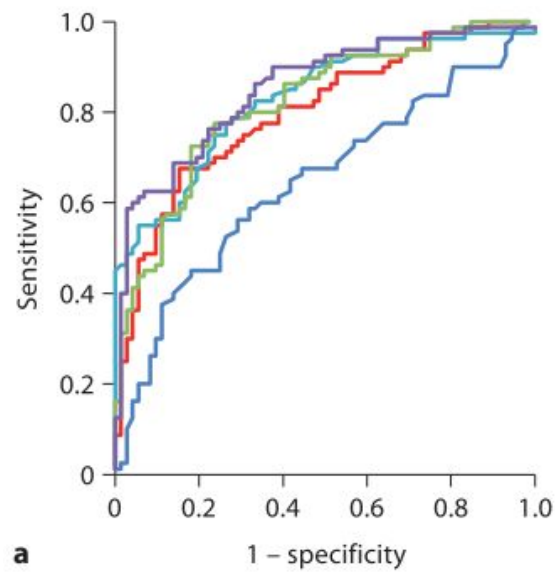


Fig.14

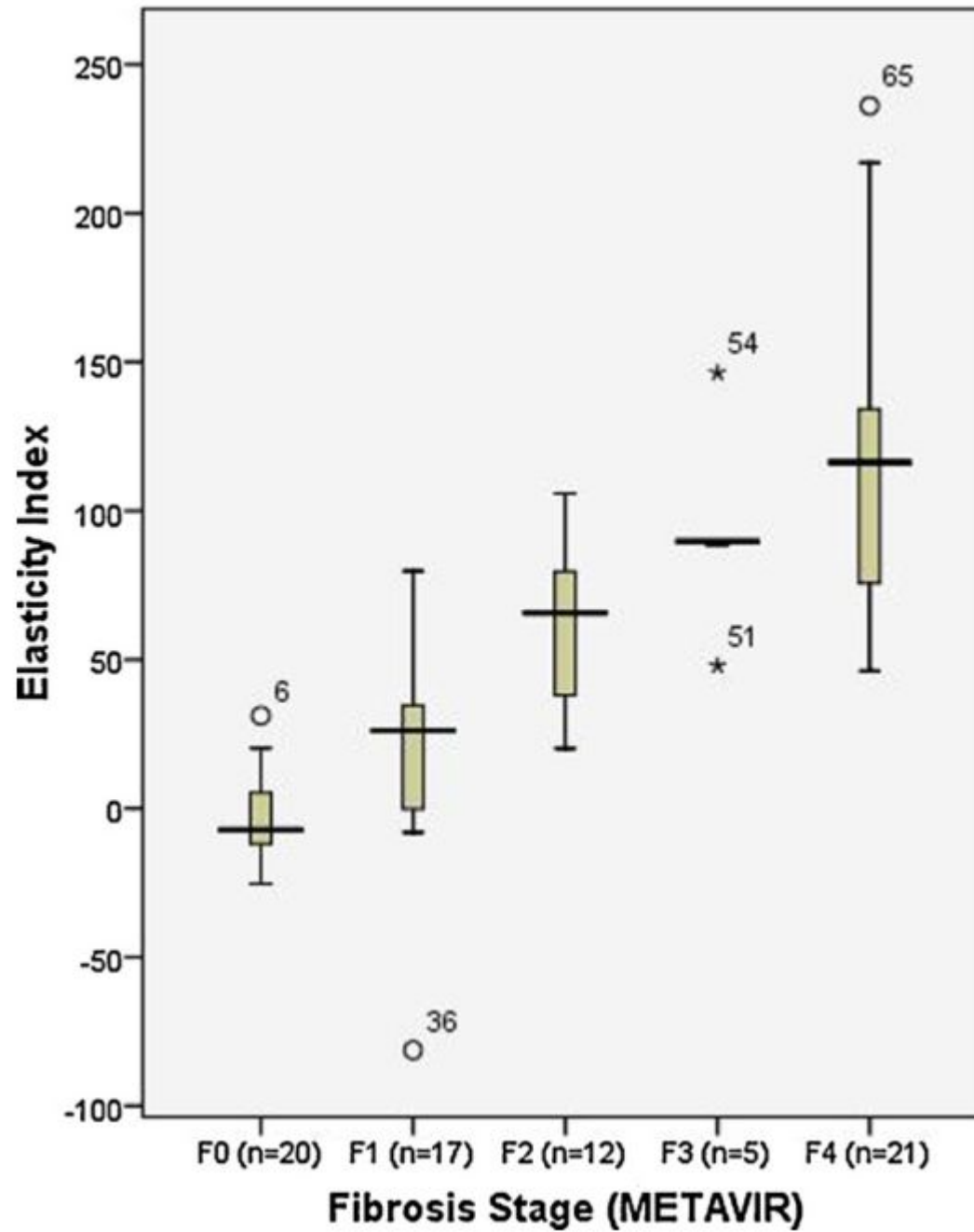


Fig.15

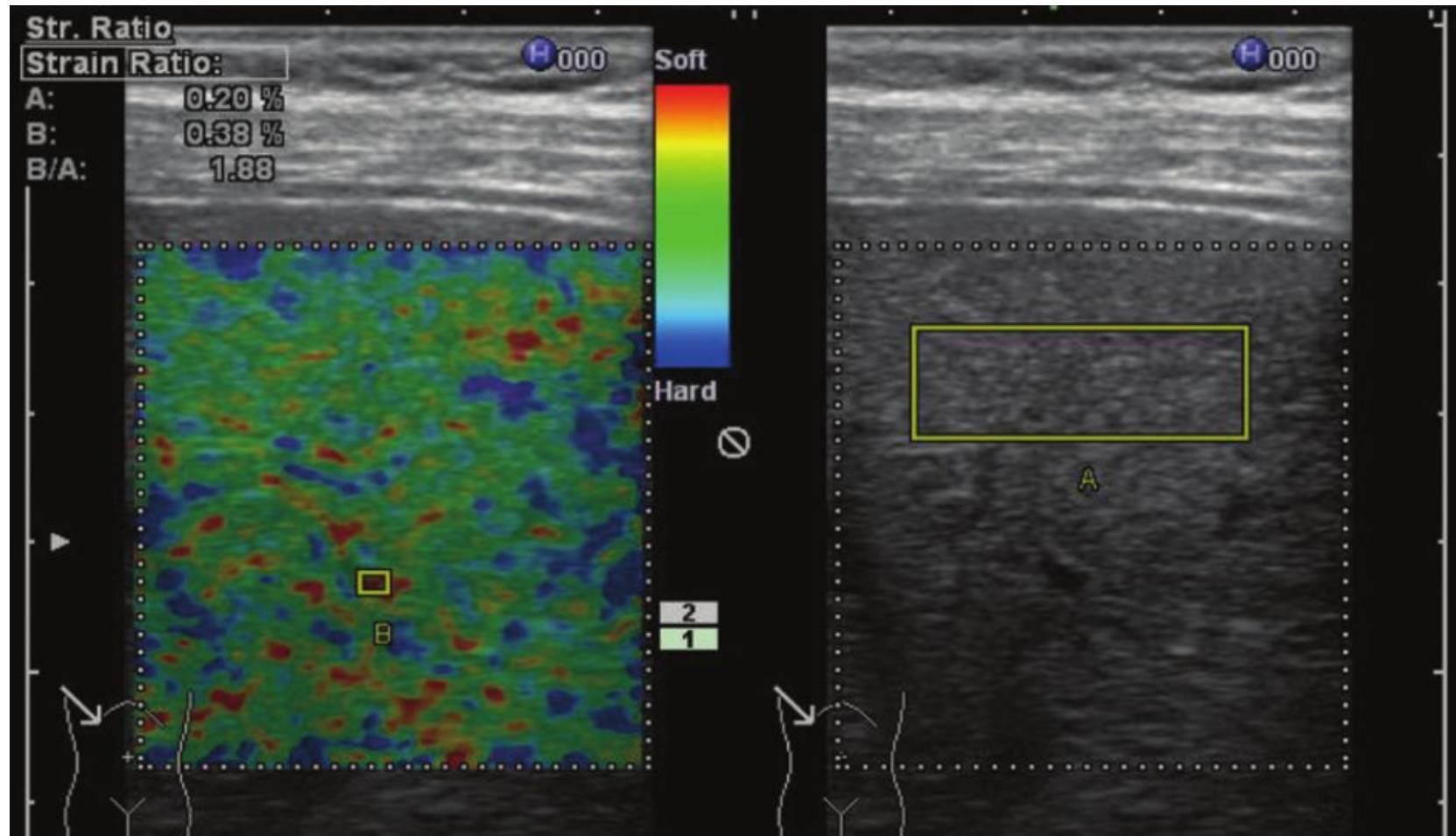


Fig.16

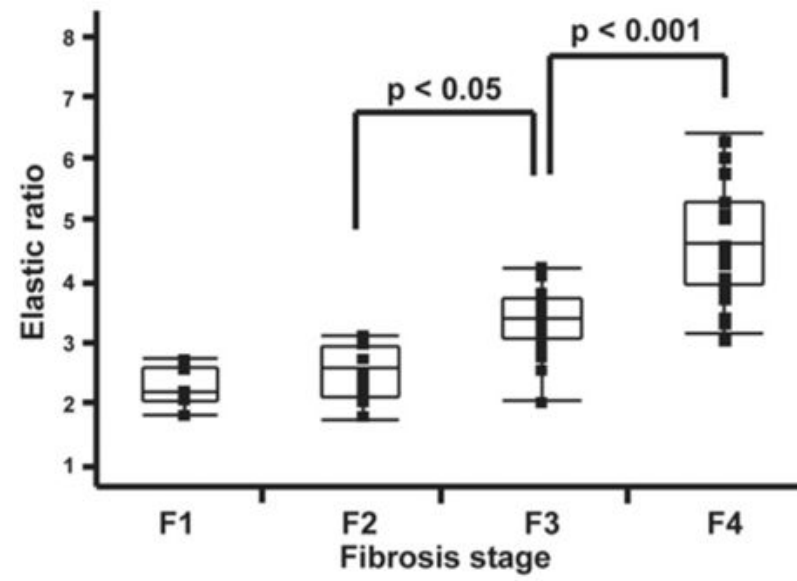


Fig.17

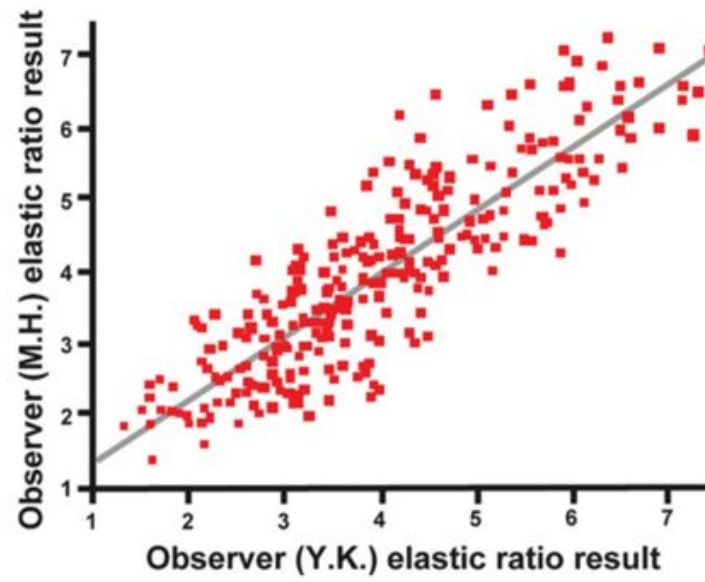


Fig.18

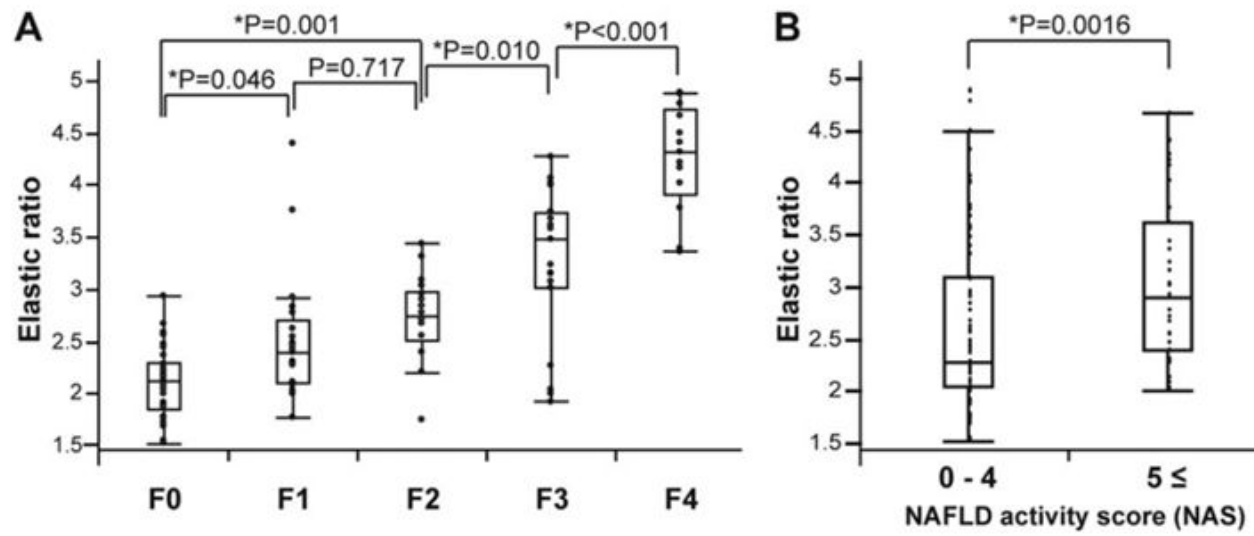


Fig.19

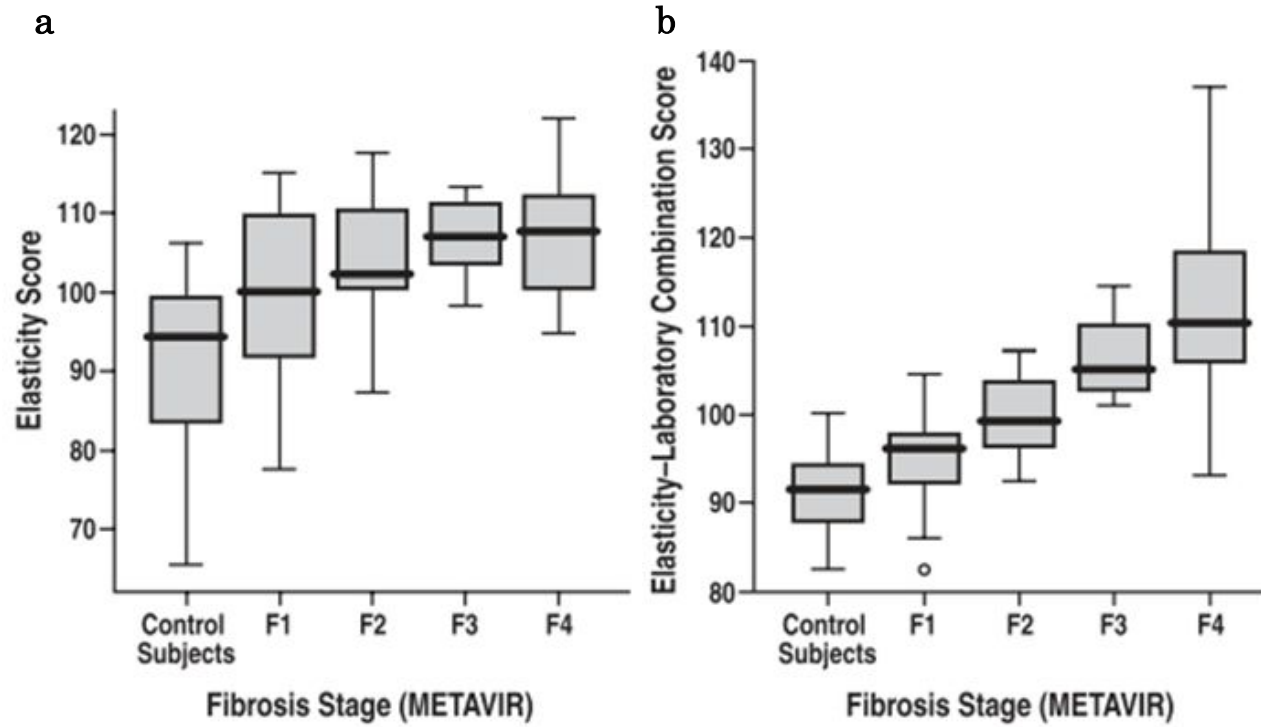


Fig.20

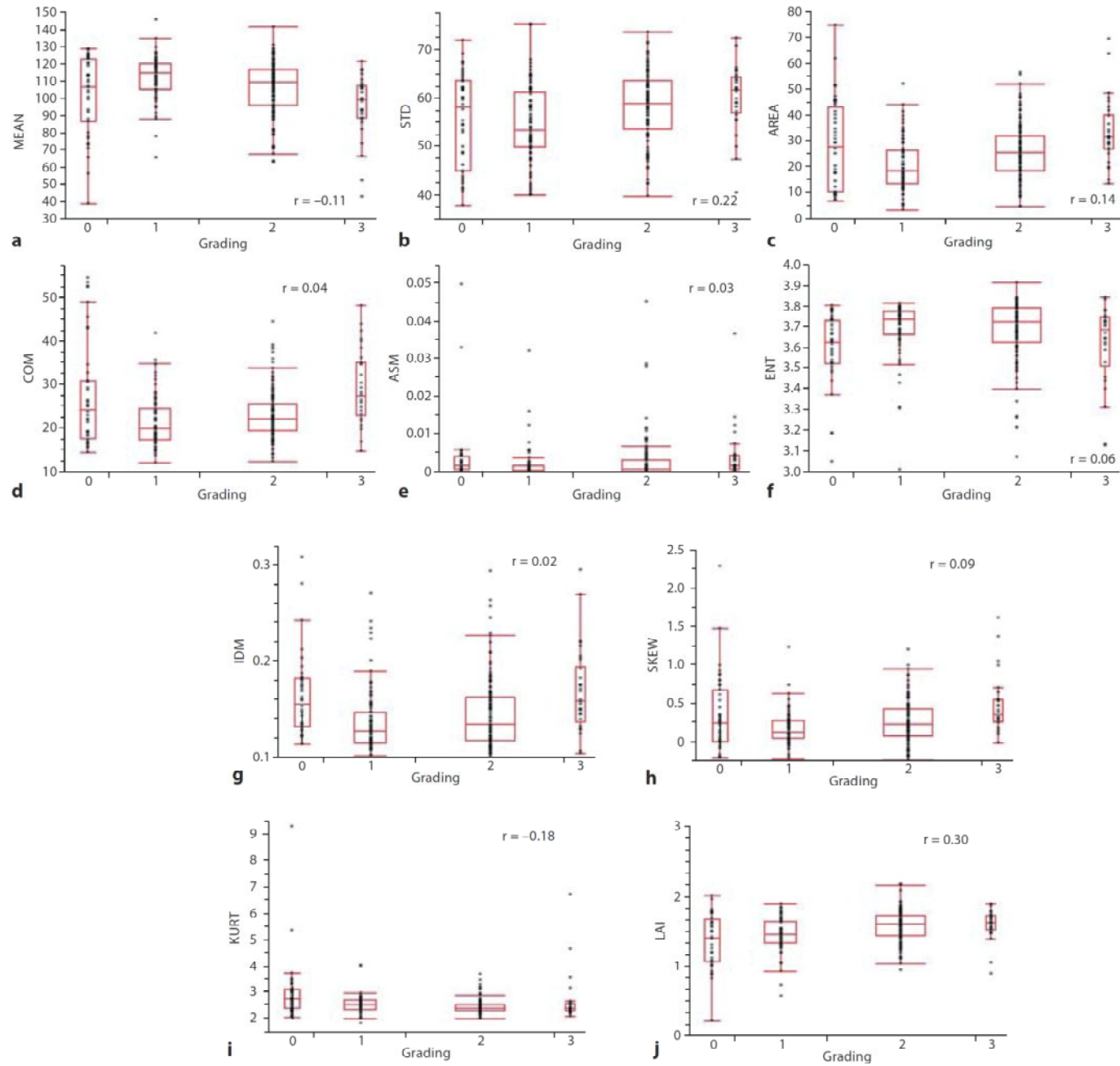


Fig.21

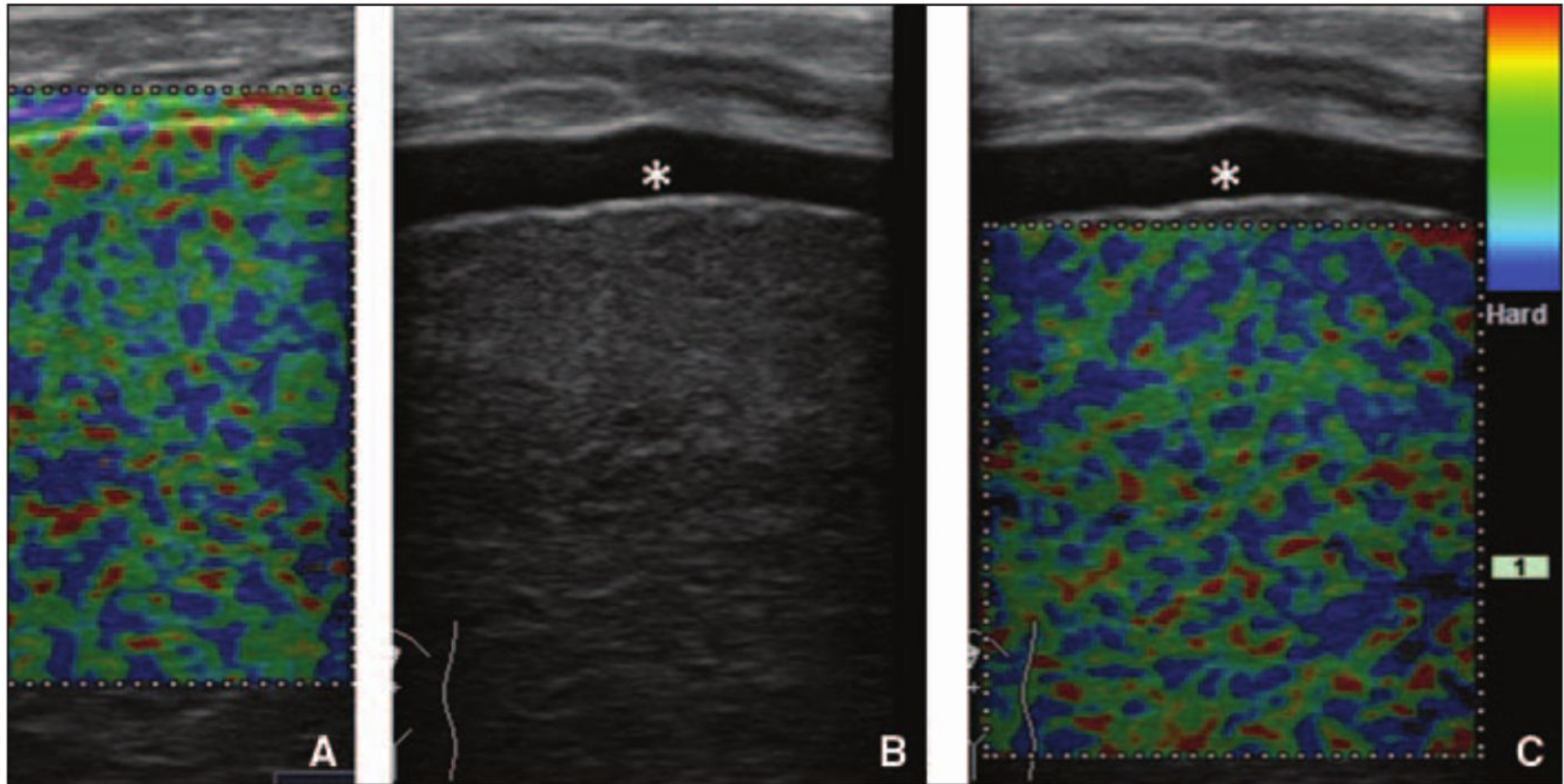


Fig.22



Fig.23

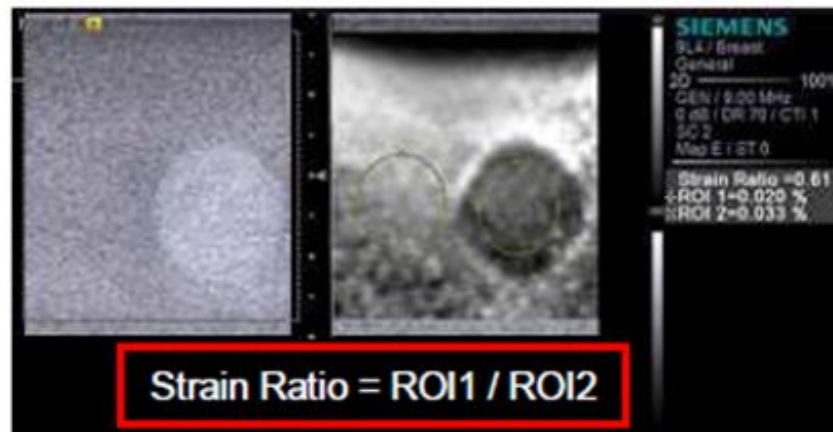


Fig.24

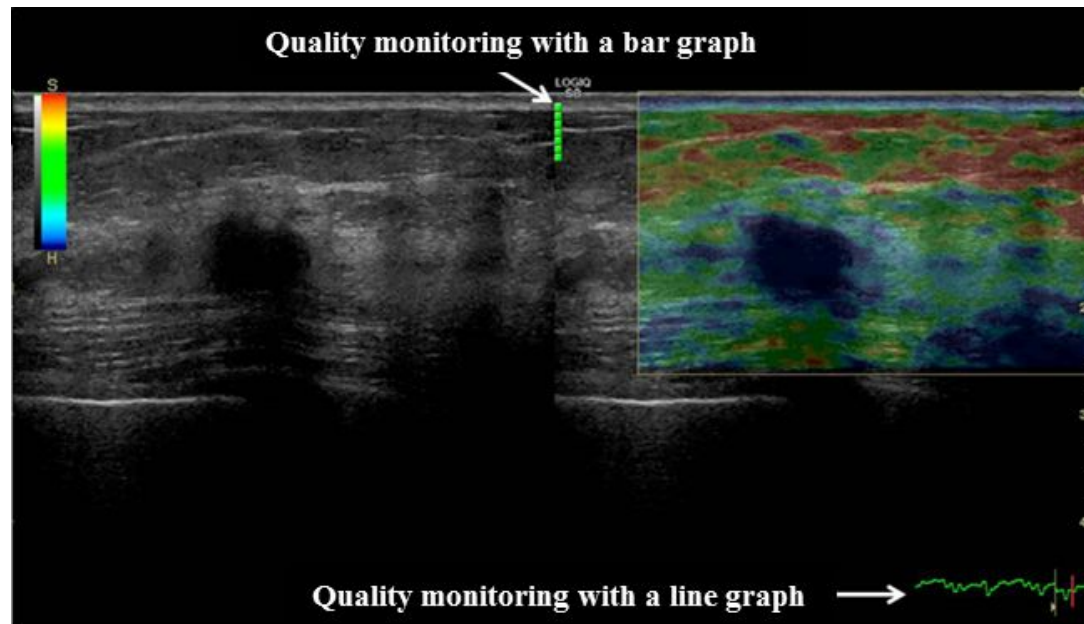
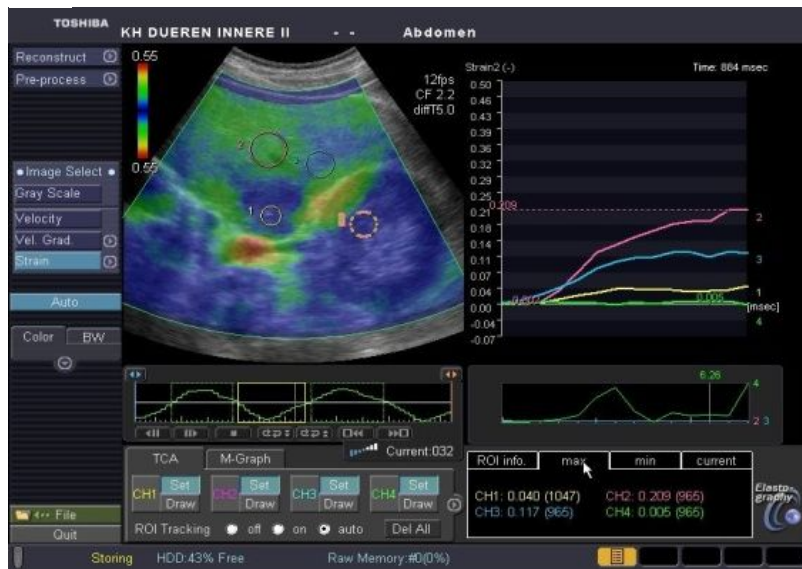


Fig.25

a



b

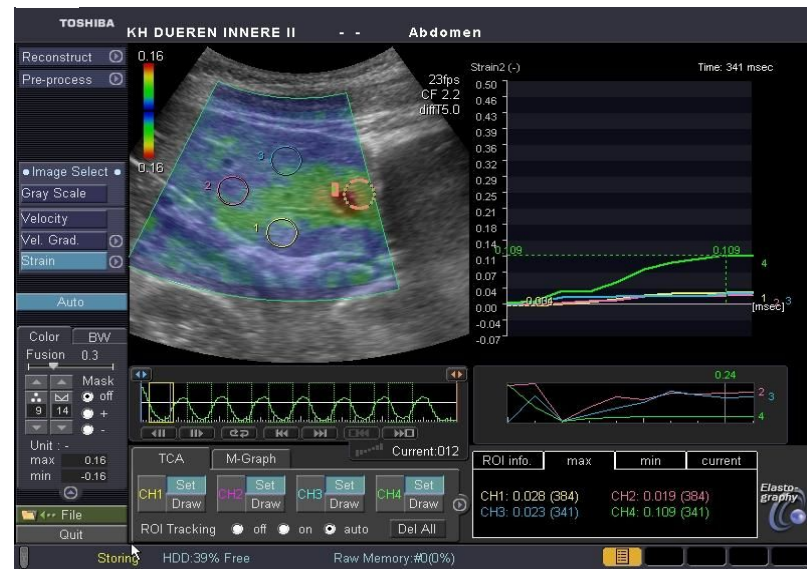


Fig.26

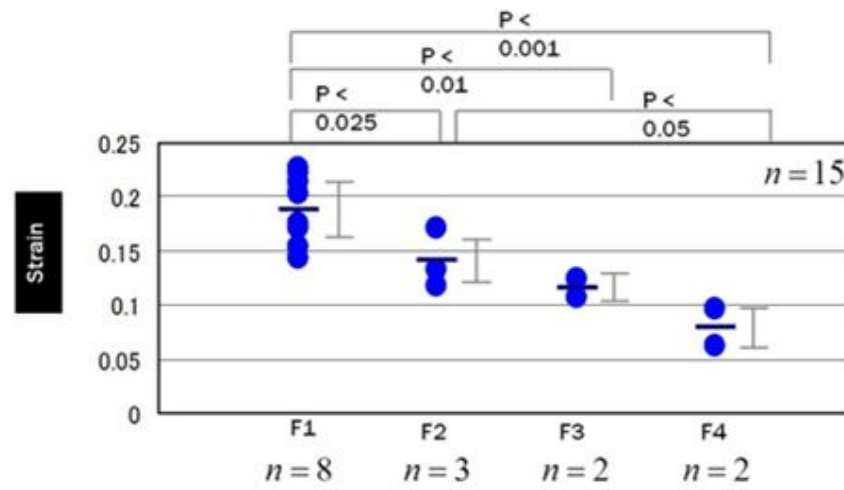


Fig.27

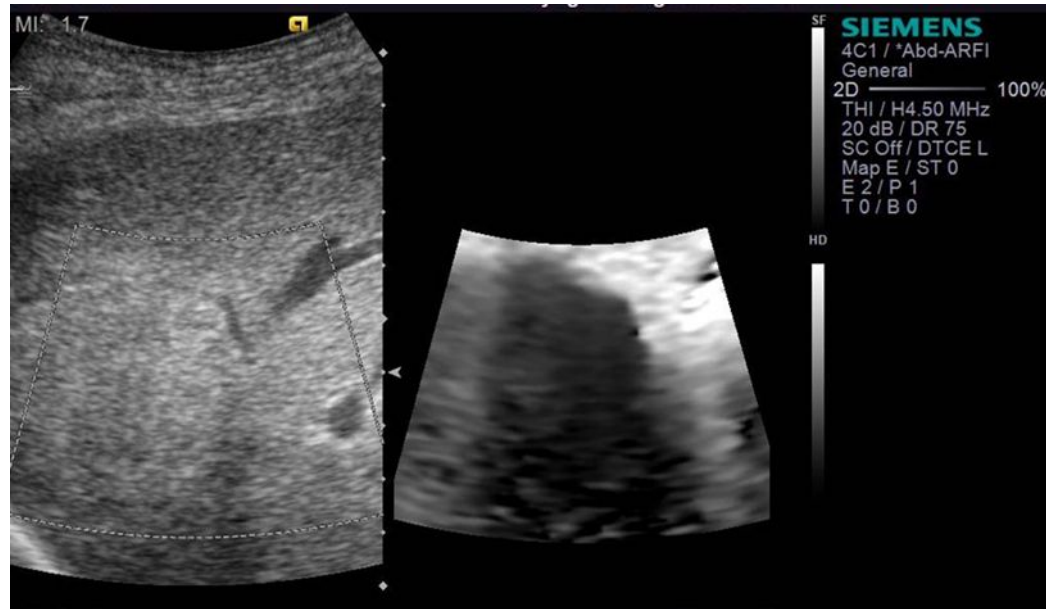


Fig.28

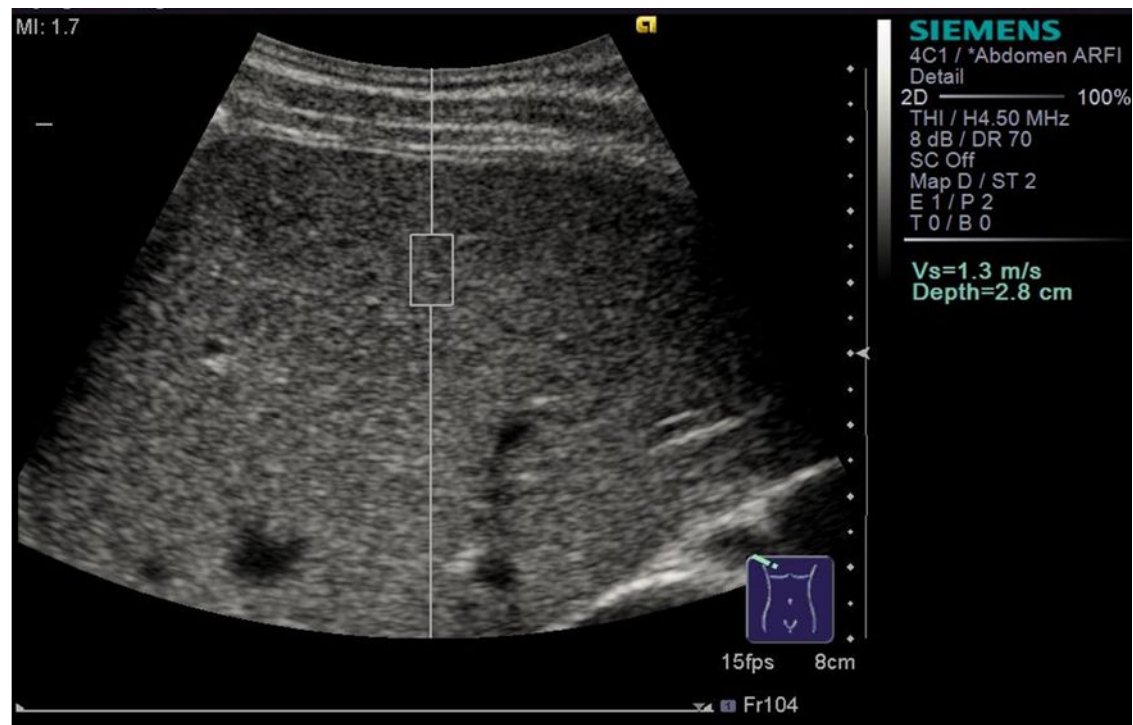


Fig.29

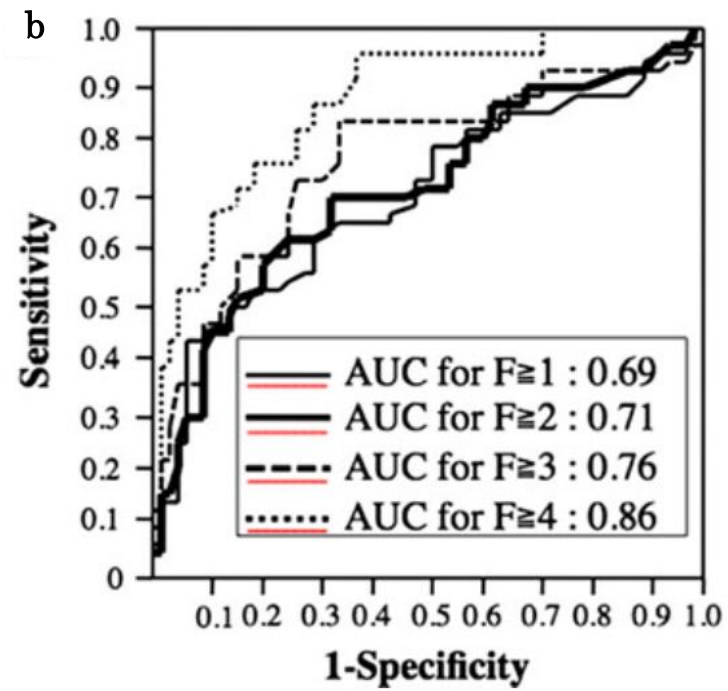
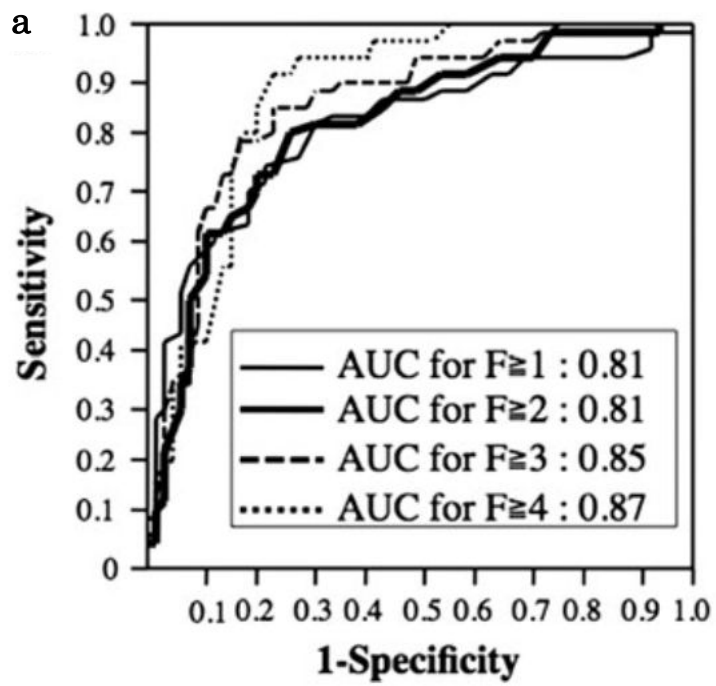


Fig.30

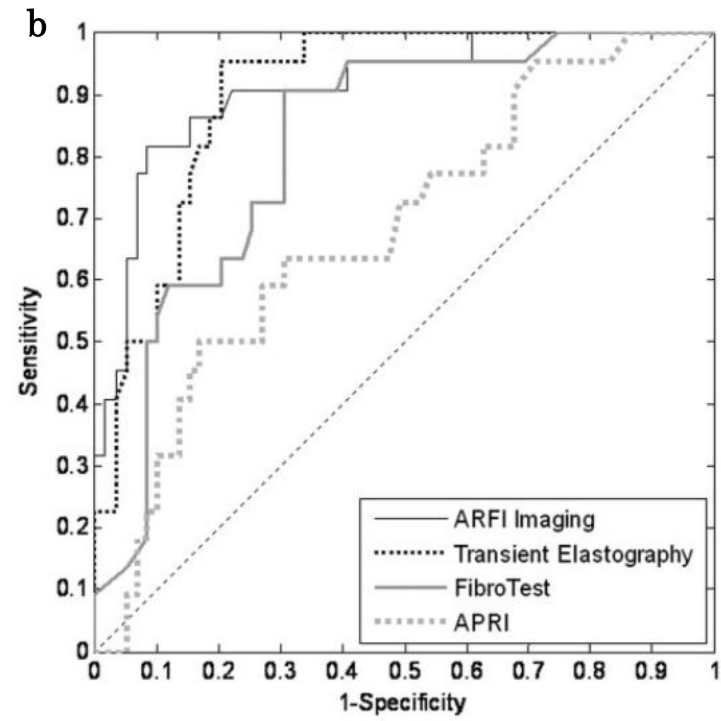
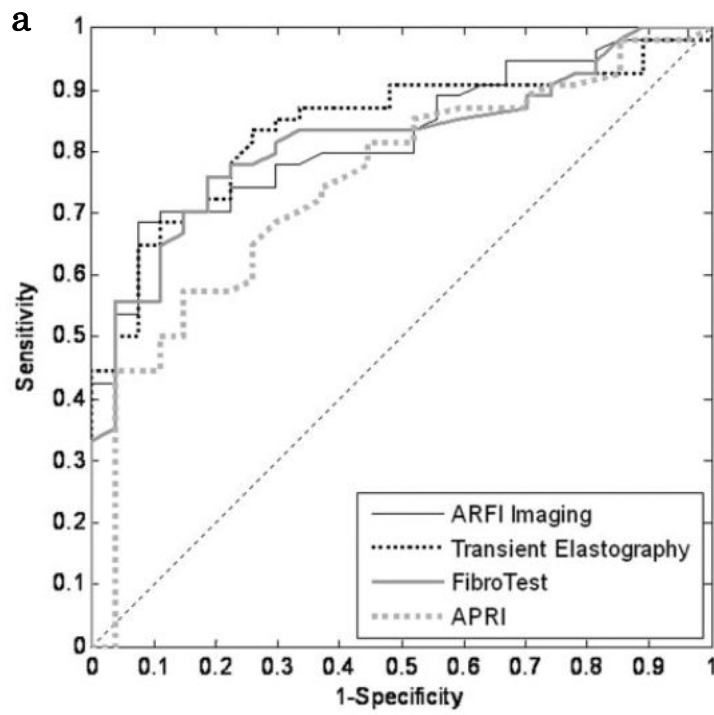


Fig.31

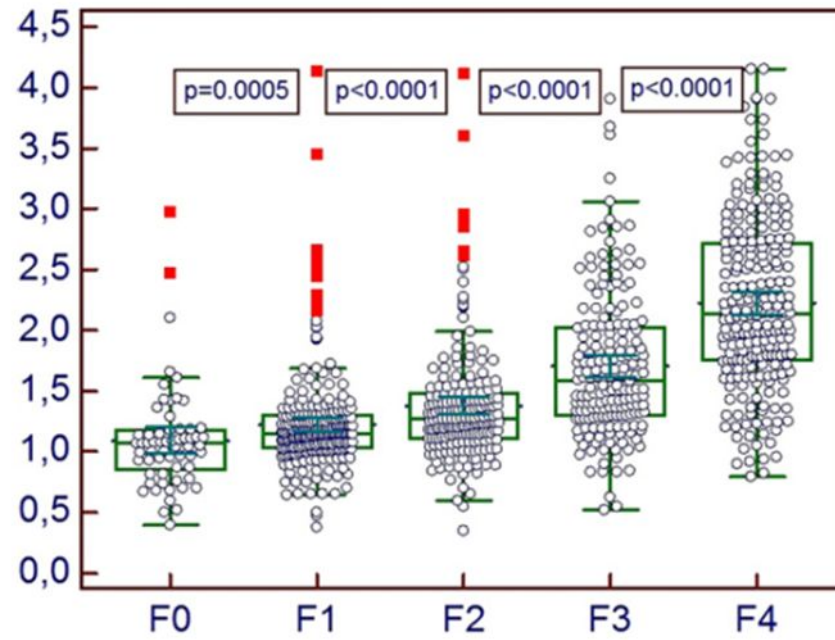


Fig.32

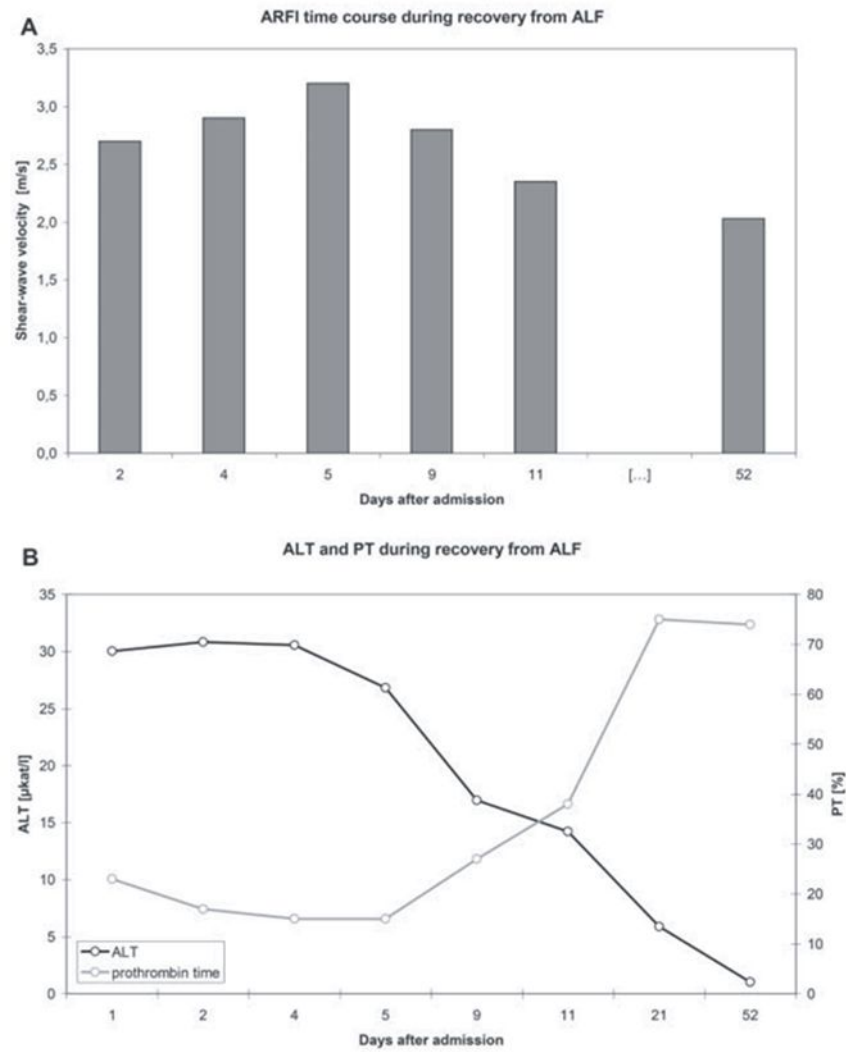


Fig.33



Fig.34

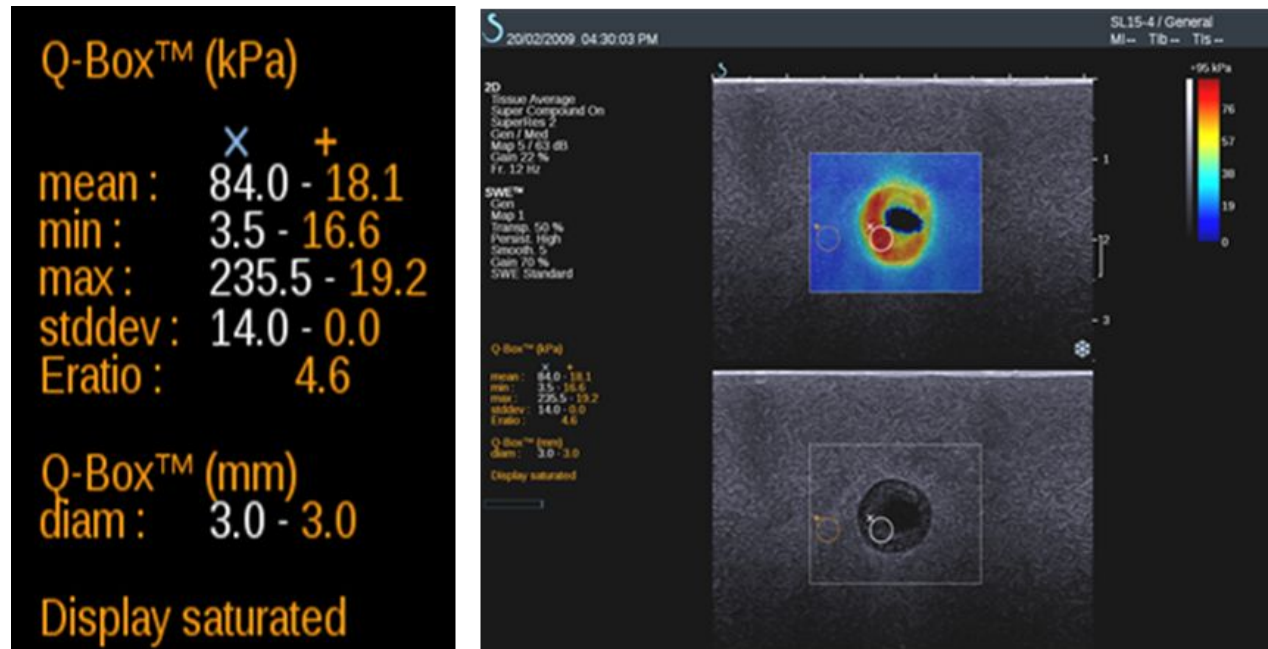


Fig.35

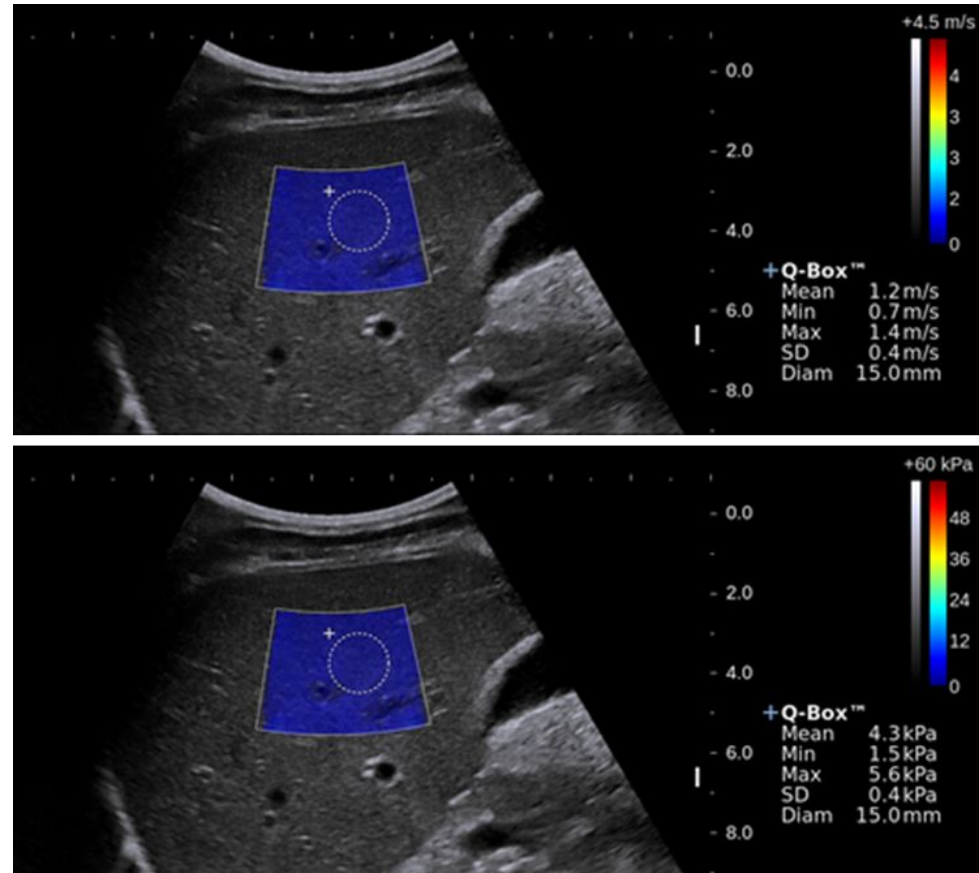


Fig.36

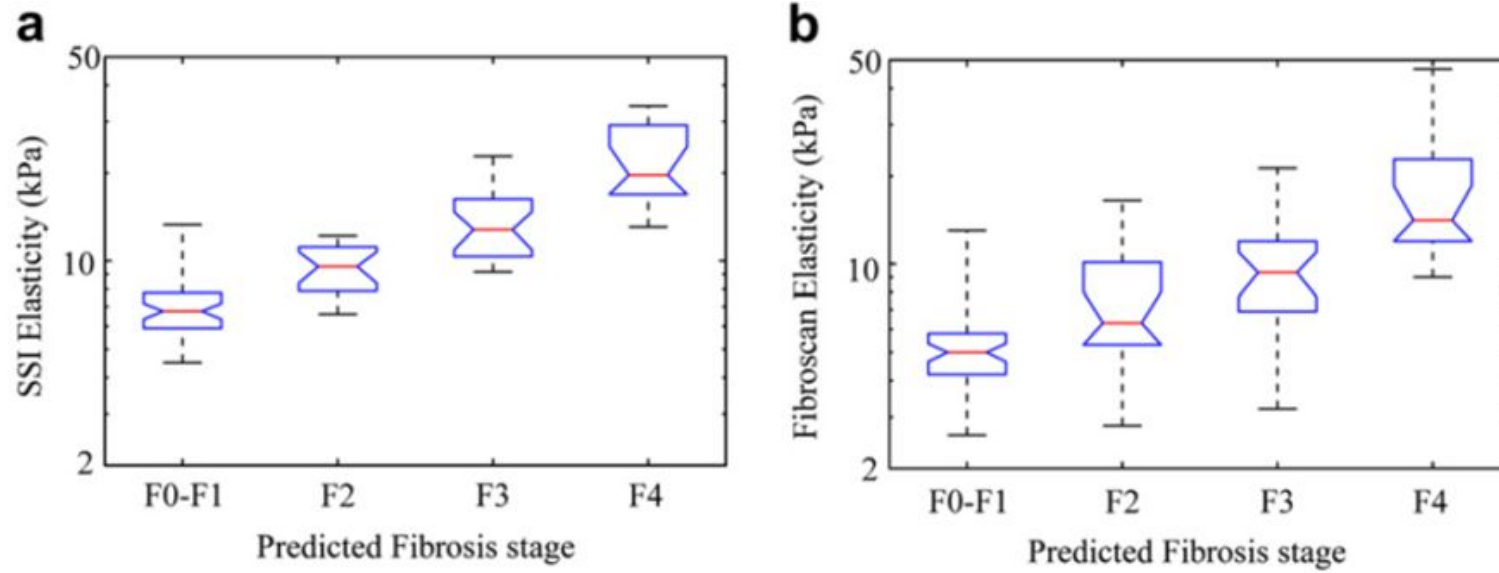


Fig.37

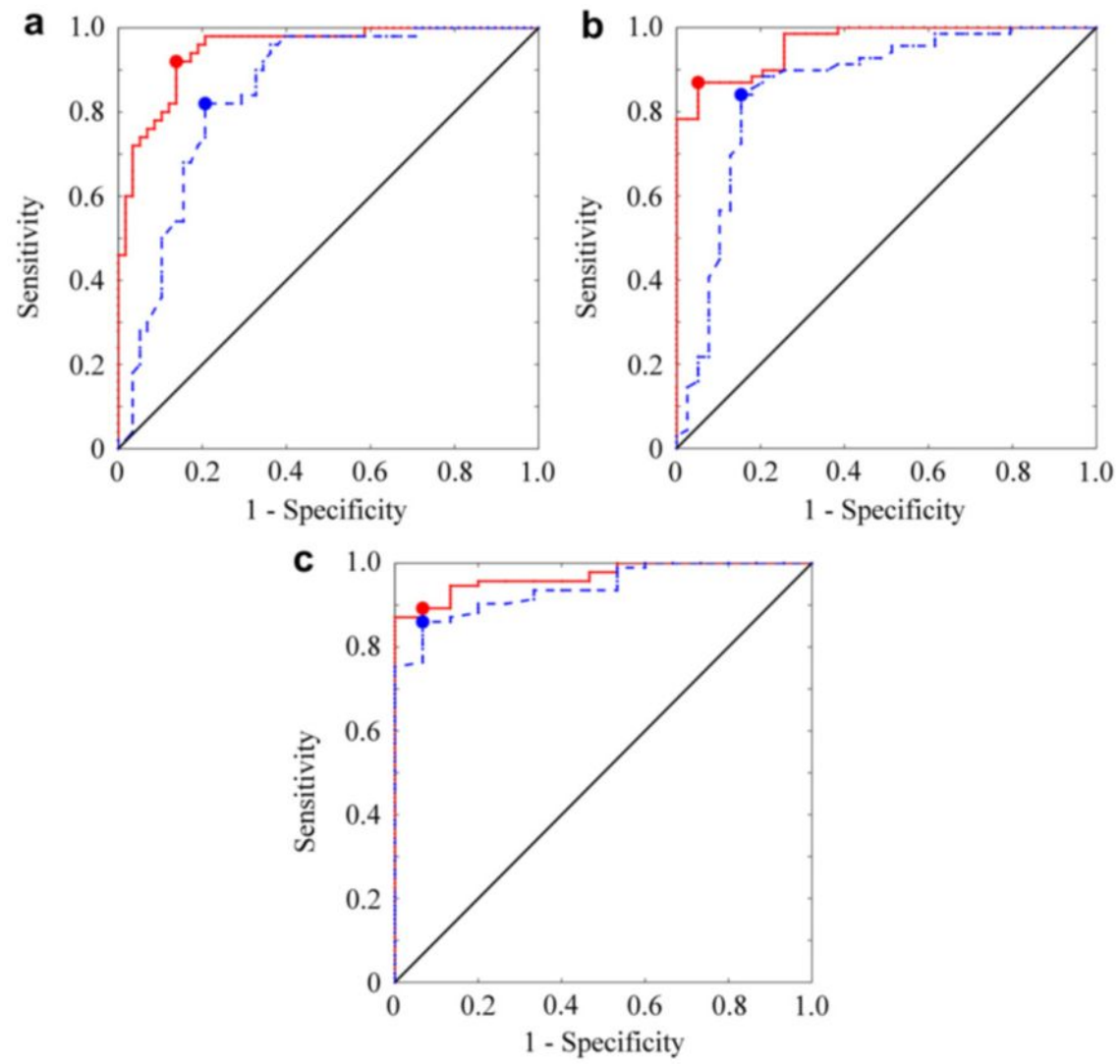


Fig.38

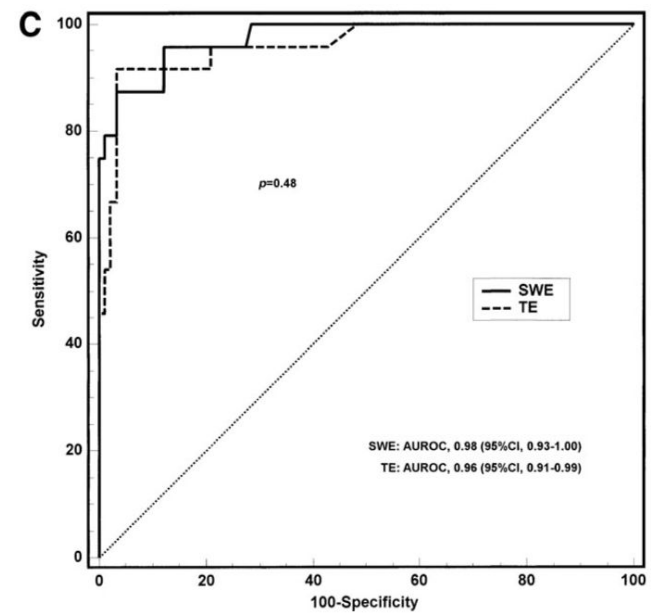
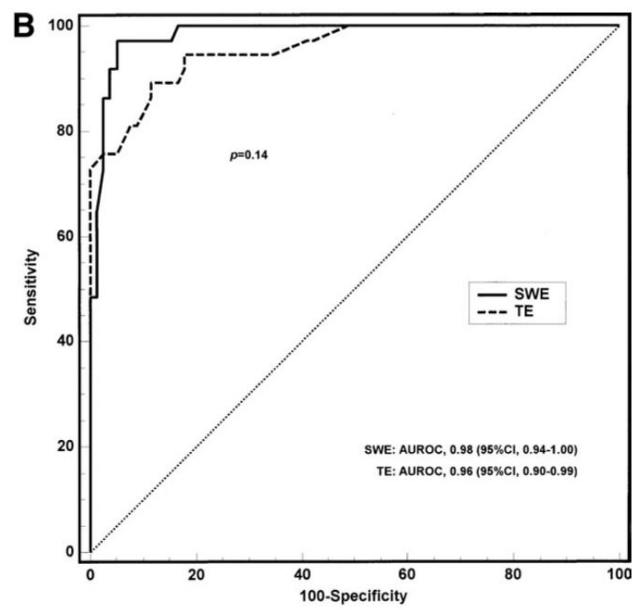
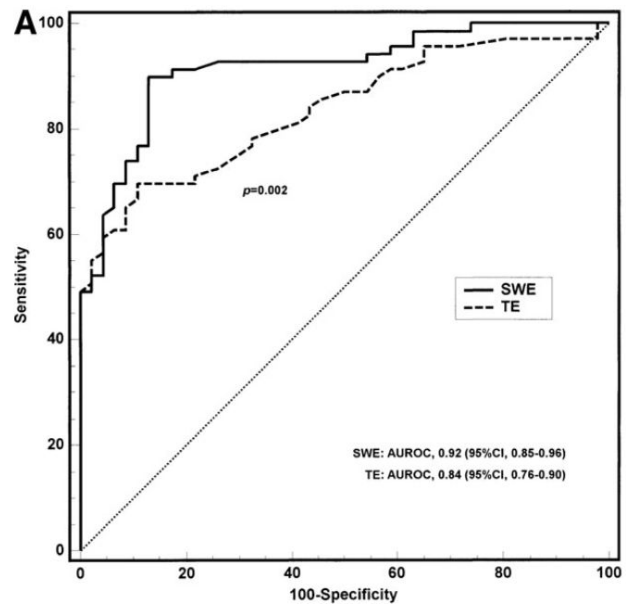


Fig.39

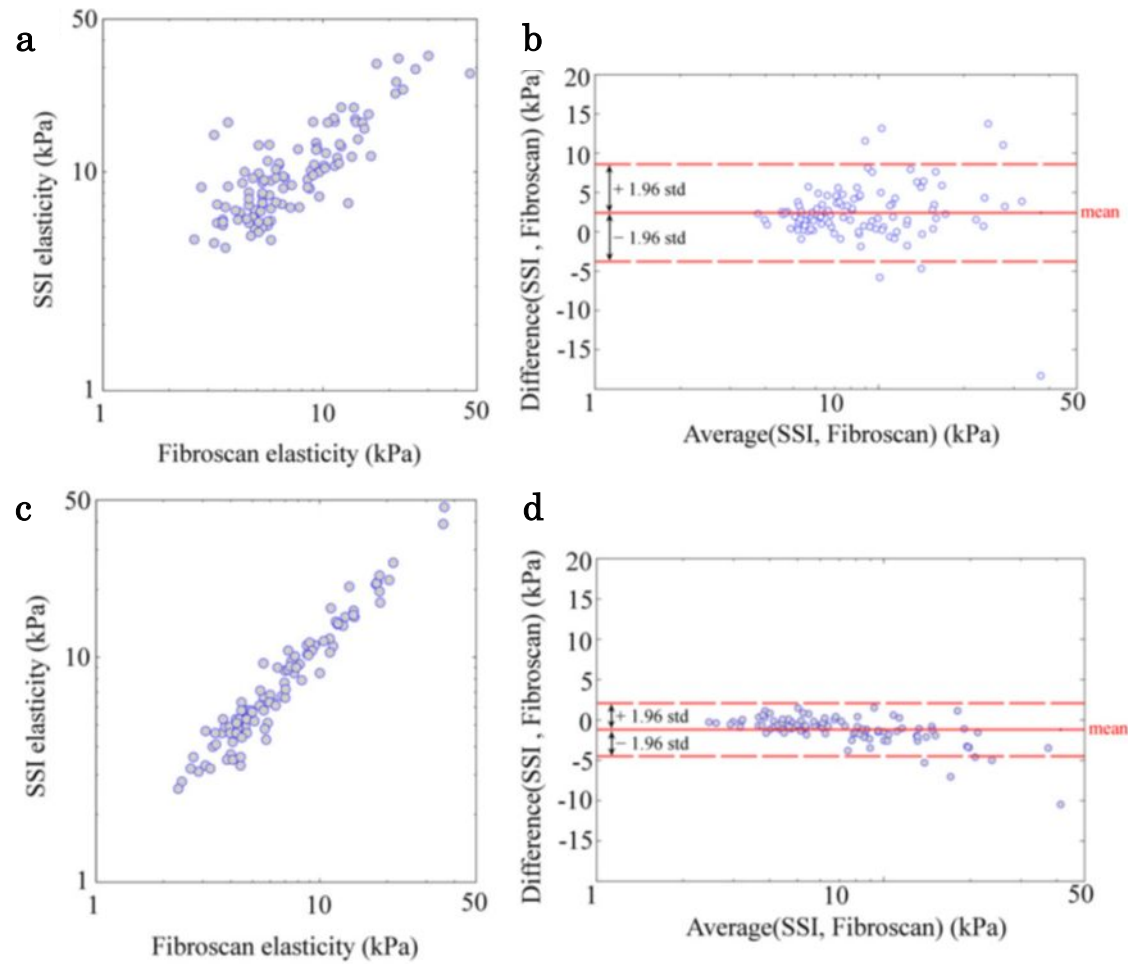


Fig.40

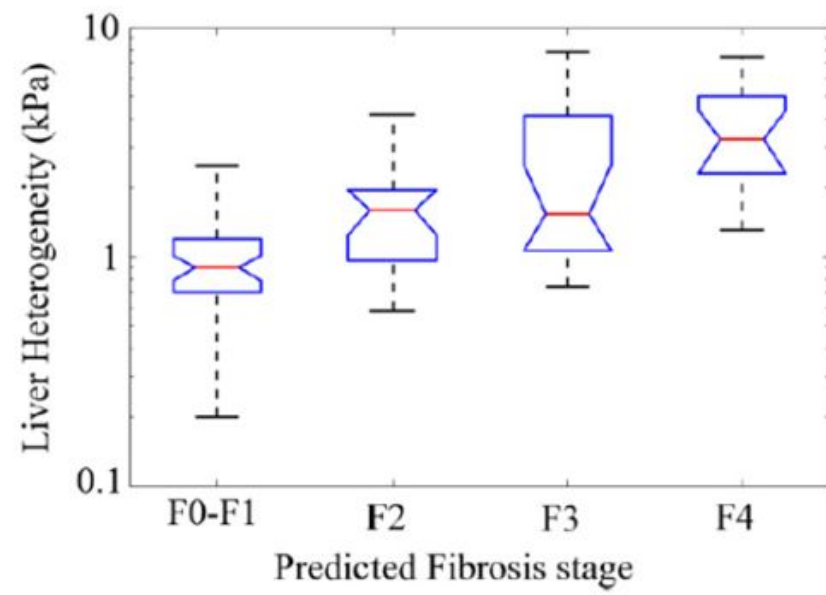


Fig.41

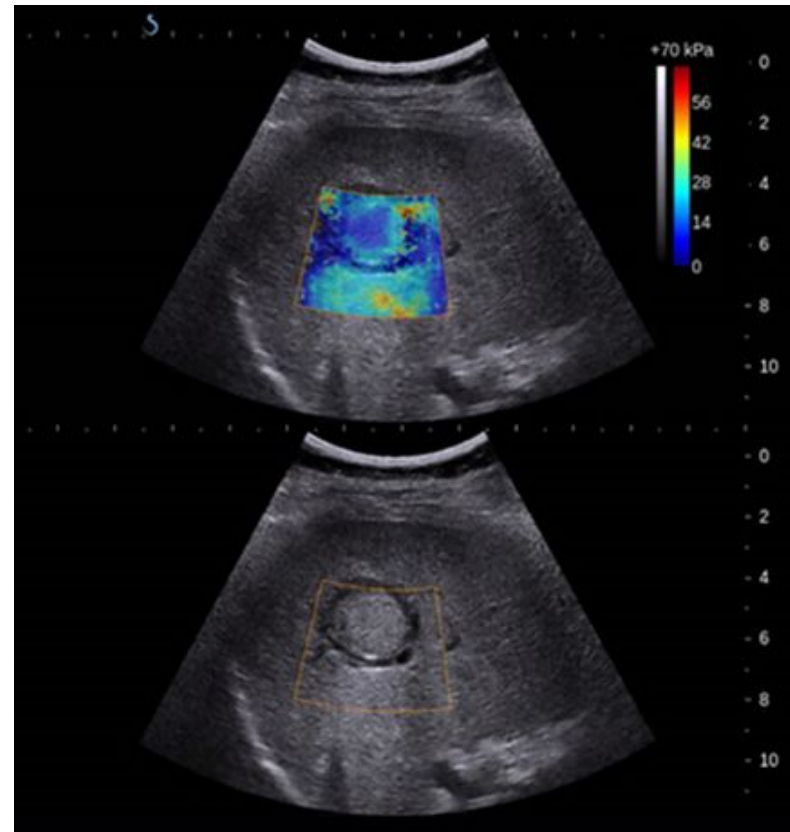


Fig.42

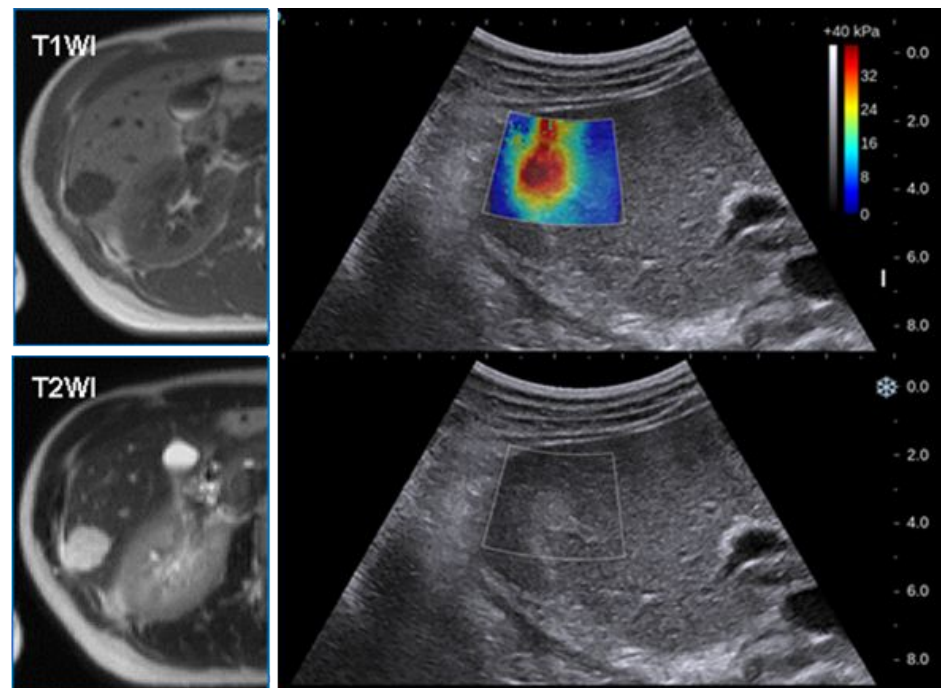


Fig.43

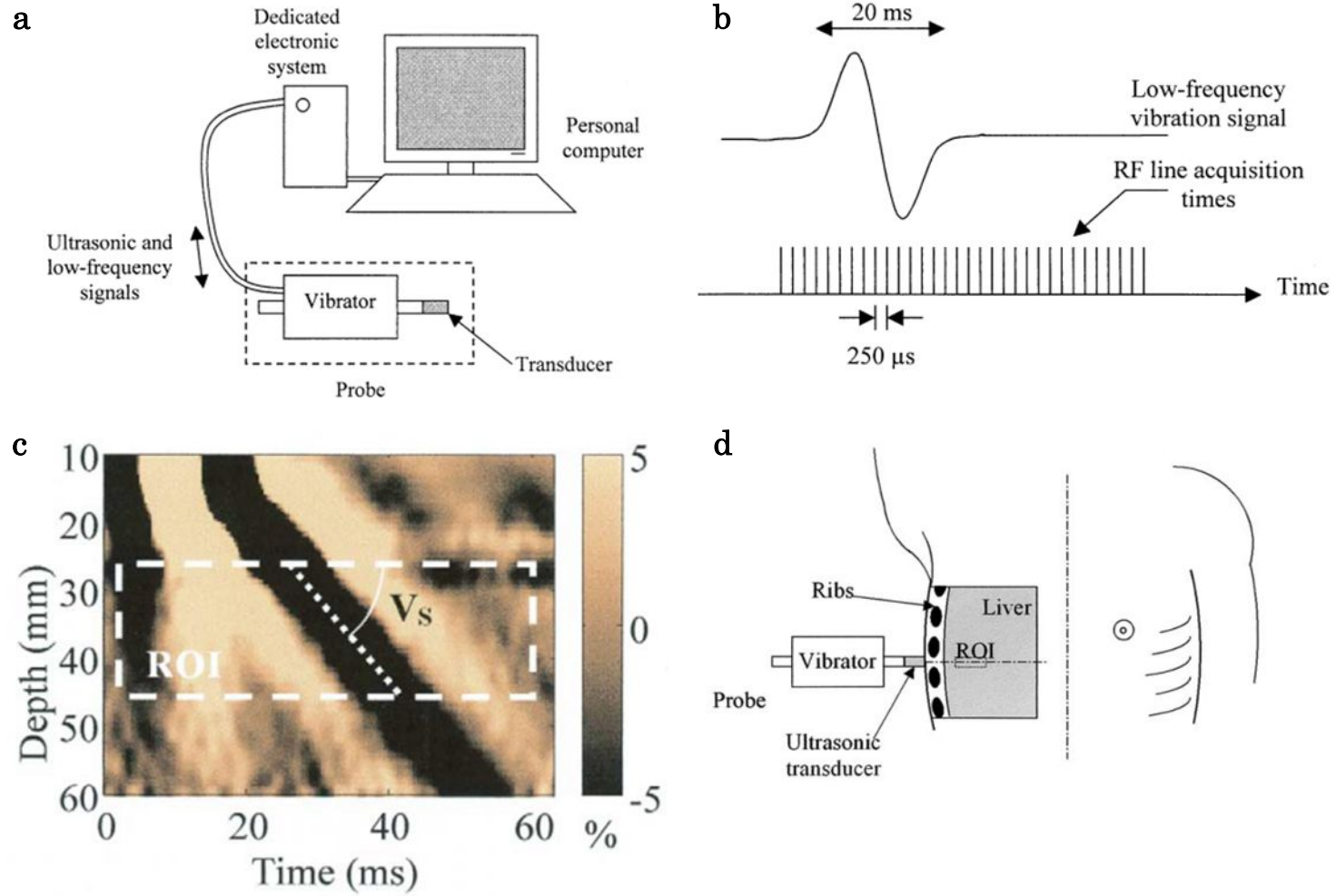


Fig.44

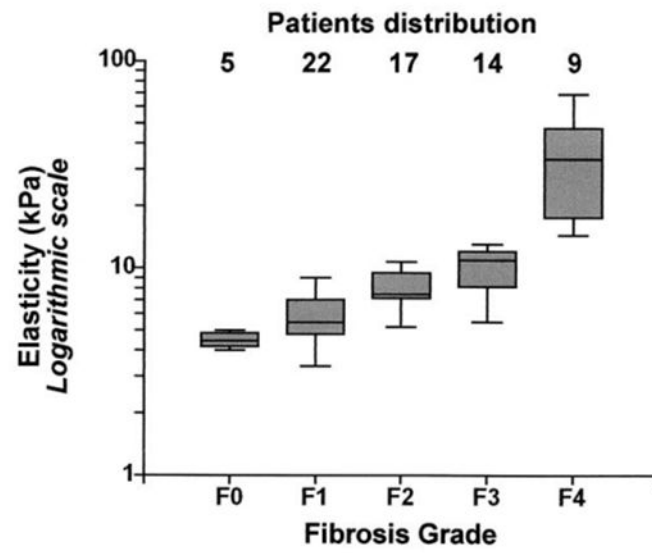


Fig.45

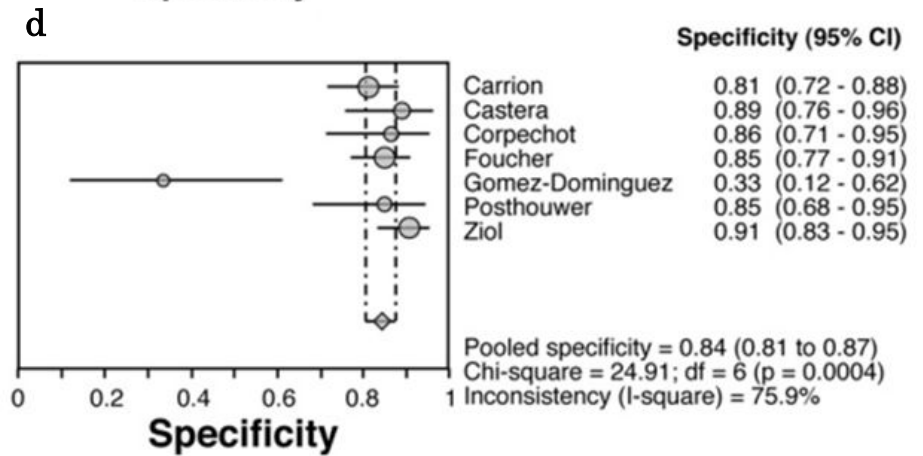
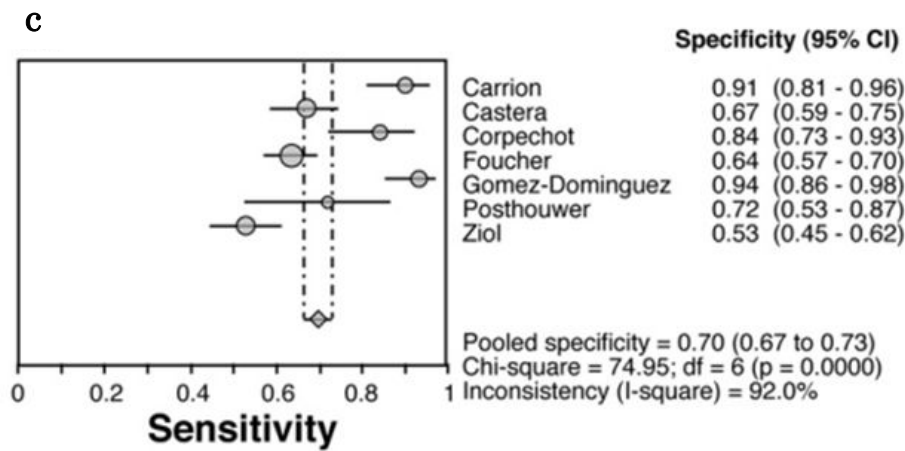
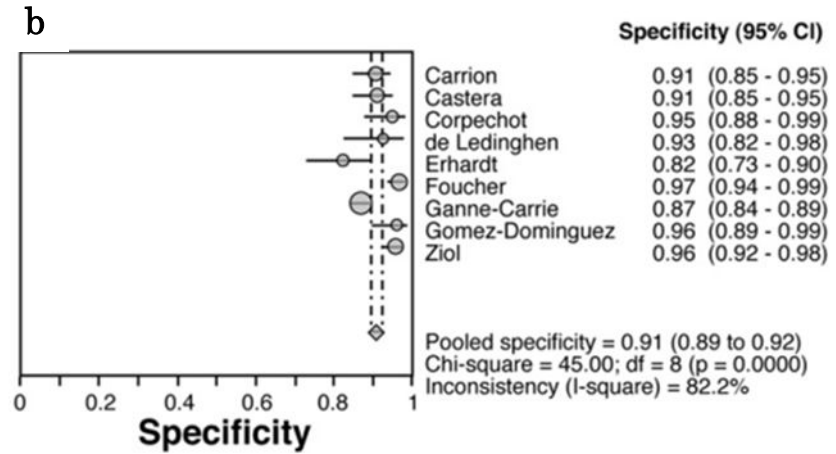
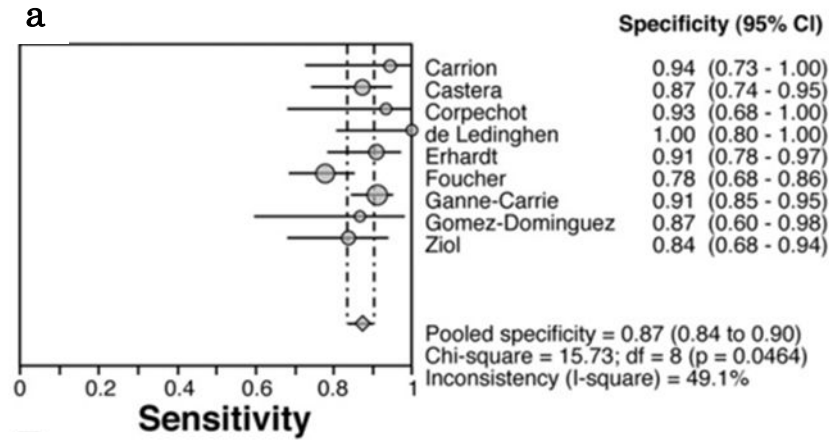


Fig.46

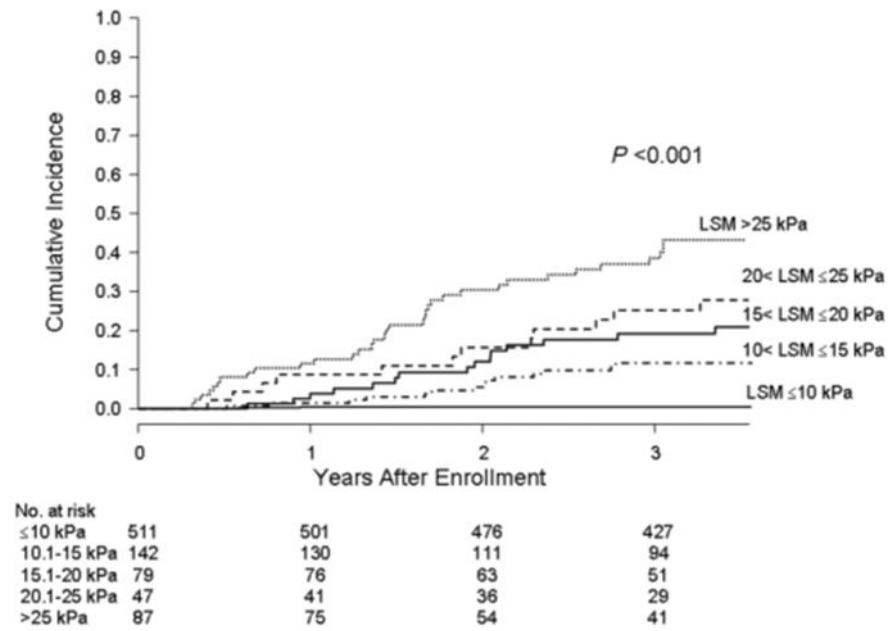


Fig.47

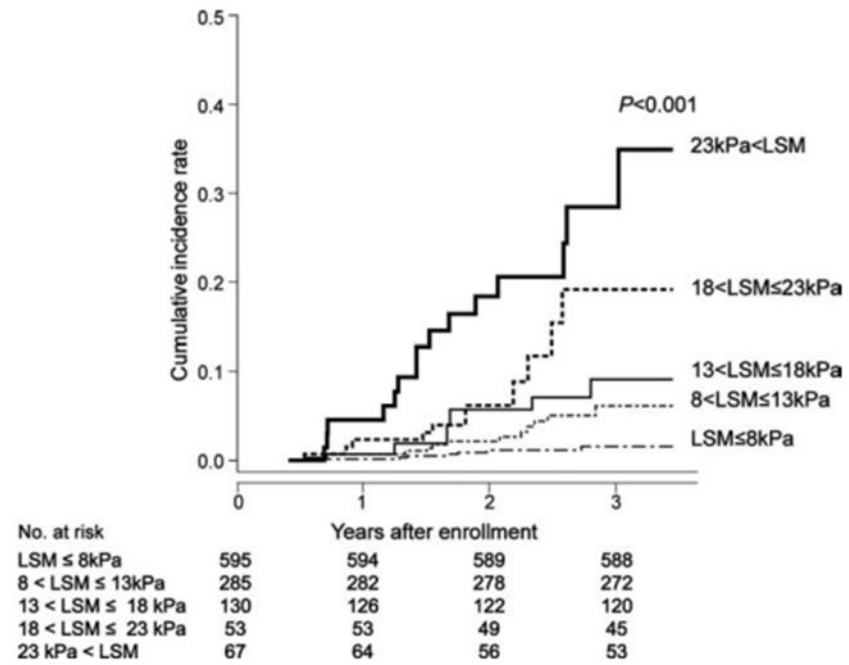


Fig.48

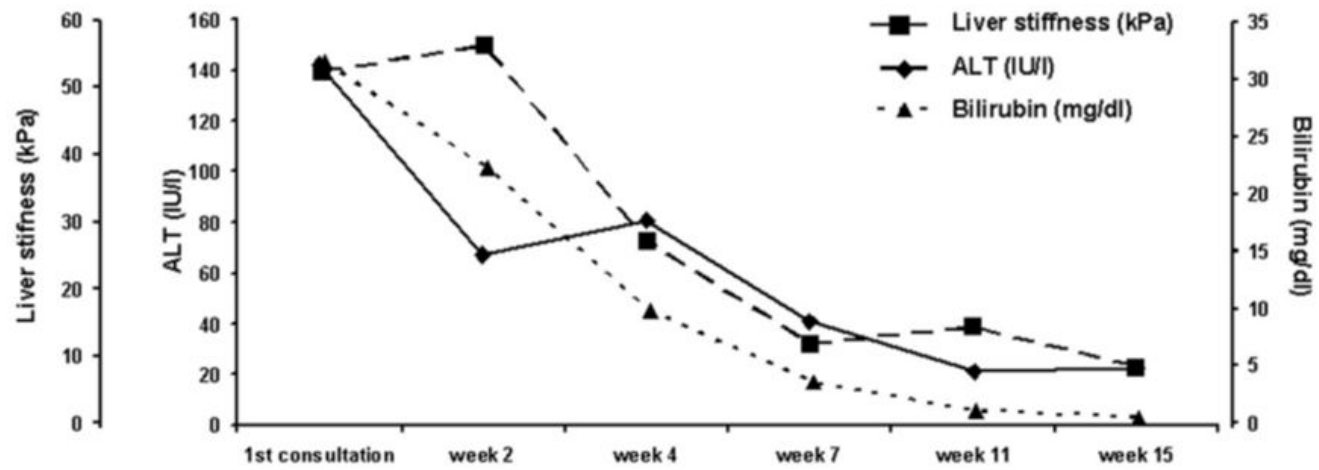


Fig.49

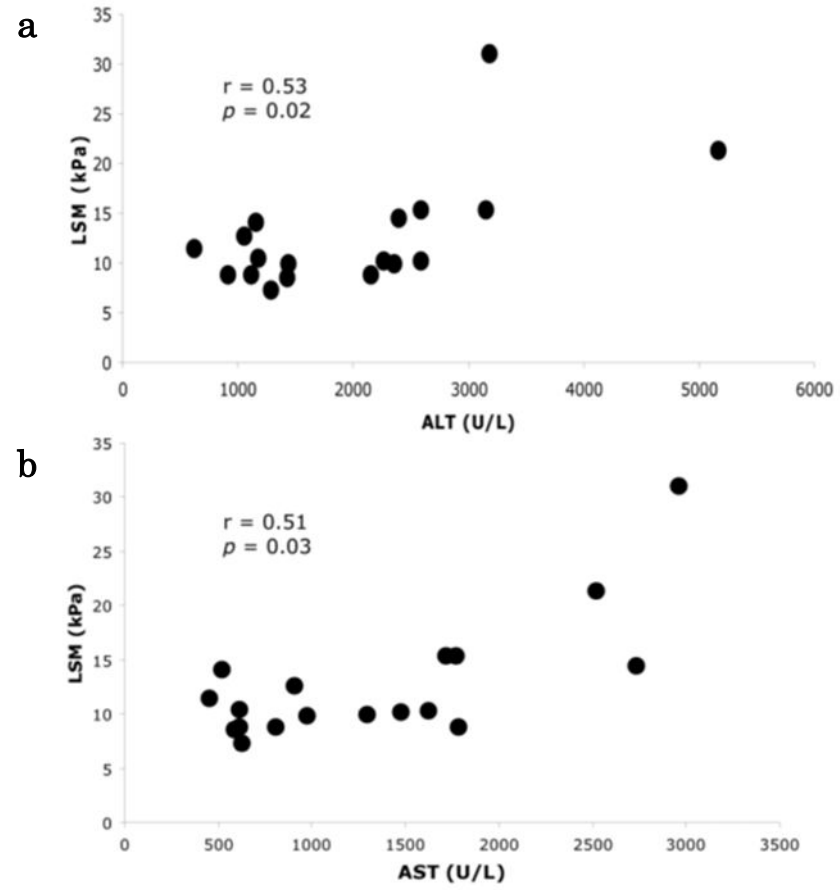


Fig.50

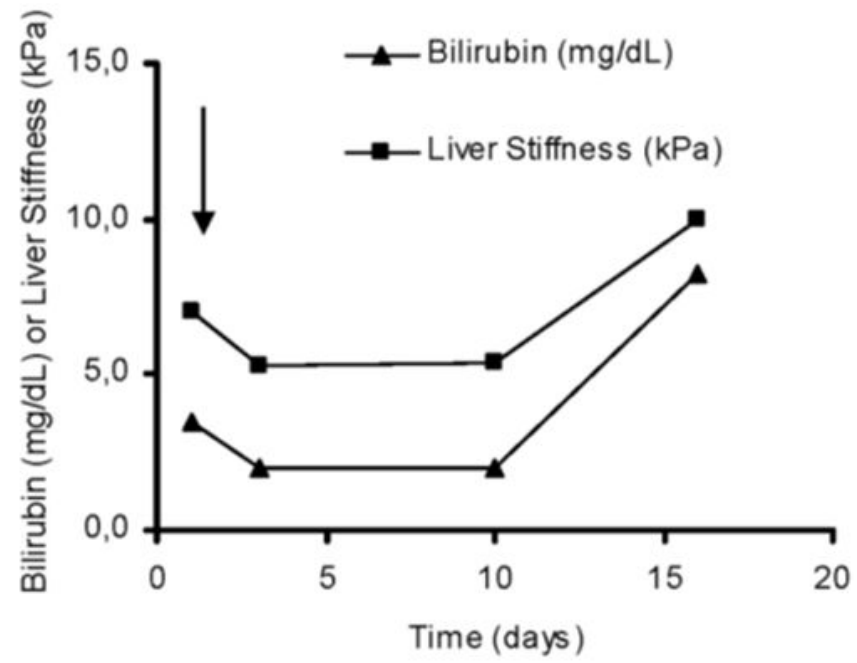


Fig.51

